

**ISTANBUL TECHNICAL UNIVERSITY**  
**FACULTY OF SCIENCE AND LETTERS**  
**GRADUATION PROJECT**



**INVESTIGATION OF SUPERCONDUCTING STRUCTURES USING  
MULTIPHYSICS MODELLING**

**Roni Can Şahin**

**Department :Fizik Mühendisliği Bölümü**

**Student ID :090160114**

**Advisor :Doç. Dr. Seda Aksoy Esinoğlu**

**SPRING 2022**

## TABLE OF CONTENTS

<b>TABLE OF CONTENTS .....</b>	<b>2</b>
<b>LIST OF FIGURES .....</b>	<b>3</b>
<b>SUMMARY .....</b>	<b>5</b>
<b>1. INTRODUCTION.....</b>	<b>6</b>
1.1 Superconductivity.....	6
1.2 The London Brothers' Equations.....	8
1.3 The Ginzburg – Landau Equations.....	10
1.4 Harmonic Oscillator .....	12
1.4.1 Lumped Element LC Resonator.....	12
1.4.2 $\lambda/4$ Resonator .....	13
1.4.3 External Coupling .....	13
1.5 Josephson Junctions .....	14
1.6 SQUIDs .....	15
1.7 The Transmon Qubit .....	15
1.8 Jaynes – Cummings Hamiltonian for Qubit – Resonator Couple .....	17
<b>2. COMPUTATIONAL .....</b>	<b>18</b>
2.1 Superconducting Disk in a Magnetic Field with London Brothers' Approach.....	18
2.2 Meissner Effect with Ginzburg – Landau Approach .....	22
2.3 Meissner Effect with Easier Approach to Boundary Conditions .....	24
2.4 Simulation of Current Carrying Superconducting Wires .....	26
2.5 Flowing Current in Thin Superconducting Strips .....	28
2.6 Creating Single Flux Quantum Pulses Using COMSOL .....	30
2.7 Cloning Single Flux Quantum Pulses Using COMSOL .....	32
2.8 Transmon Qubit in a Coplanar Waveguide Cavity .....	33
<b>3. RESULTS &amp; DISCUSSION.....</b>	<b>35</b>
<b>4. CONCLUSION &amp; OUTLOOK .....</b>	<b>40</b>
<b>5. REFERENCES.....</b>	<b>41</b>

## LIST OF FIGURES

Figure 1 External field H where $H < H_c$ . When temperature is higher than $T_c$ , a) shows the magnetic flux has no effect. When Temperature cooled down below critical temperature $T_c$ , b) superconductor expels magnetic flux but c) perfect conductor's flux remain same. ....	6
Figure 2 Electron - Phonon interaction where the electron 1 and electron 2 are forming a Cooper Pair .....	7
Figure 3 H - T phase diagrams for a) Type I superconductor b) Type II superconductor.....	8
Figure 4 Schematic of transmon qubit, superconducting island and reservoir by josephson junctions.Resonator is coplanar waveguide resonator. ....	16
Figure 5 Disk in a magnetic field with London Brothers' Approach parameters at COMSOL Multiphysics interface.....	19
Figure 6 Geometry of Superconducting Disk and the box on COMSOL Multiphysics GUI.....	20
Figure 7 Coefficients From PDE defined as shown on COMSOL Multiphysics for the case of superconducting disk on a magnetic field with London Brothers' approach simulation .....	21
Figure 8 Result of the superconducting disk on a magnetic field with London Brothers' approach simulation.....	21
Figure 9 Input Parameters for Meissner Effect with Ginzburg-Landau Approach simulation on COMSOL Multiphysics .....	22
Figure 10 a)Equation for the real part of the wave function where =u, b) Equation for the imaginary part of the wave function .....	22
Figure 11 a) Equation for Ax b) Equation for Ay.....	23
Figure 12 Vortex pattern at t=200s .....	23
Figure 13 Parameters are the same as before, but R and r are added .....	24
Figure 14 Here the vol function is defined in COMSOL.....	25
Figure 15 TDGL Equations with vol function inserted in COMSOL GUI .....	25
Figure 16 Evolution of vortices for the time at t=200s on COMSOL GUI .....	26
Figure 17 Parameters for the 1D Superconducting wire in COMSOL GUI.....	26
Figure 18 TDGL Equations are written as follows in COMSOL GUI .....	27
Figure 19 Cooper pair density at top, normal current at bottom and superfluid current at the middle showing that their change with respect to time in COMSOL GUI.....	28
Figure 20 Parameters for the relevant simulation and the 2D geometry of the thin film in COMSOL GUI.....	28
Figure 21 TDGL Equations for Thin Film Superconductivity .....	29
Figure 22 Flow of the electric current in the superconductors cause vortice pattern .....	29
Figure 23Superconductor-Normal metal-Superconductor junction [9] .....	30
Figure 24 Parameter to create SFQ pulse on SNS junction on COMSOL GUI .....	30
Figure 25 TDGL Equations of the relevant simulation on the COMSOL GUI.....	31
Figure 26 SFQ Generation on SNS junction at time t=100s in COMSOL GUI.....	31
Figure 27 Parameters used .....	32
Figure 28 TDGL Equations for cloning the SFQ Pulses on COMSOL GUI.....	32
Figure 29 3D Working Geometry in COMSOL GUI .....	33
Figure 30 Plane Geometry of the qubit-cavity coupler circuit .....	33
Figure 31 Mesh Geometry .....	34
Figure 32 Mesh Geometry showing down part and the cross section between up and down geometries .....	34

Figure 33 Meissner effect in superconducting disk using London Brothers' Approach.....	35
Figure 34 Meissner Effect on Superconducting Disk in a magnetic field using TDGL equations .....	35
Figure 35 Close - up of the figure 34.....	36
Figure 36 Formation of the simulation of Meissner Effect using TDGL Equations where showing the time at t=0, 20.4s, 28.4s, 33.2s, 51.3s and 120s.....	36
Figure 37 Evolution of the vortices using TDGL Equations with boundary conditions at time t=0, 10s, 18s, 21.2s, 65.2s, 185.5s.....	37
Figure 38 Cooper Pair Density (Top), Normal Current (Bottom) and Supercurrent (Middle) with time at t=0, 13.86 and 21.92s.....	37
Figure 39 Cooper Pair Density with respect to time at t =0, 0.9s, 1.8s, 21.3s, 30.7s and 37s....	38
Figure 40 Formation of the SFQ Pulse respect to time.....	38
Figure 41 Electric field map of the system .....	39
Figure 42 S Parameters of the system.....	39

# **INVESTIGATION OF SUPERCONDUCTING STRUCTURES USING MULTIPHYSICS MODELLING**

## **SUMMARY**

Superconductivity is a unique phenomenon that has gathered a huge attention in the fields of physics and engineering regarding to its unique specifications and potential applications. At below critical temperature, some materials show zero electrical resistance and obtain ability to expel external magnetic fields which results possibility for lossless electrical conduction that can be used to develop lots of different technologies such as medical imagining, energy storage and high speed trains.

In this thesis, we used a simulation software that takes advantage of the power of the finite element analysis, Comsol Multiphysics, to study the characteristic behaviours of the superconducting materials and their effects by the magnetic fields, external currents and temperature etc. Later on, we have discussed the models and analysis of these regarding to their electrical and magnetic properties and compared those results with the experimental results on the literature.

One area in the field of superconductivity has attracted significant attention especially in the last decade; superconducting qubits, which are equivalent of the classical bits on the quantum circuits that helps us to store and manipulate quantum information. By enabling these qubits and understand the true nature of them, one can develop highly precise sensors and quantum computers. At this thesis, we also use the Comsol Multiphysics to simulate superconducting qubits coupled to microwave cavities and coplanar waveguides, which are transmission lines used for carry the microwave signals.

## 1. INTRODUCTION

### 1.1. Superconductivity

Electrical resistance can be described as how easy the electricity flows on a material. In a regular conductor, copper i.e, some of the energy lost as heat while electricity flows on that material. There is a phenomenon called superconductivity, which allows the superconductors to lost no energy as heat while the electricity flows, hence zero electrical resistance.

A perfect diamagnetism, expulsion of the whole magnetic field, and zero resistance result this superconductivity phenomenon. Some materials below critical temperature  $T_c$  and critical magnetical field  $H_c$  results superconductivity and this is discovered in 1911 by H. Kammerlingh Onnes and G. Holst. They cooled down the mercury and measured the transition of superconductivity at  $T_c = 4.2$  K. [1] Later on, Meissner and Ochsenfeld proposed another characteristic of superconductors in 1933, the expulsion of the magnetic field and critical magnetic field,  $H_c$ , a phenomenon called Meissner Effect as an outcome of the zero electrical resistivity [2].

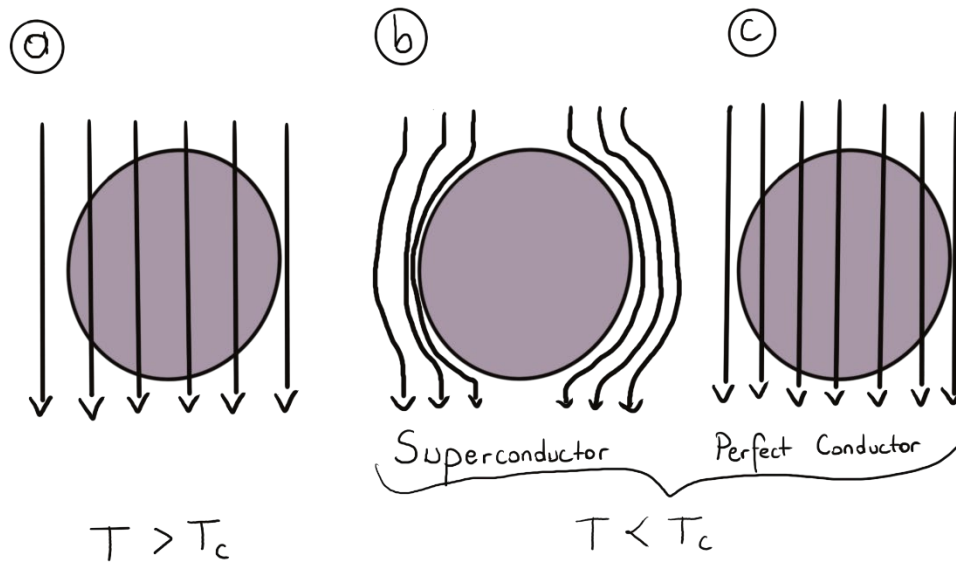


Figure 1 External field  $H$  where  $H < H_c$ . When temperature is higher than  $T_c$ , a) shows the magnetic flux has no effect. When Temperature cooled down below critical temperature  $T_c$ , b) superconductor expels magnetic flux but c) perfect conductor's flux remain same.

Bardeen, Cooper and Schrieffer proposed an excellent theory in 1957 to explain superconductors, which is famously known as BCS Theory [3, 4]. One key deficiency is that this theory only suitable for the metallic and alloy superconductors. BCS Theory is depending on the Cooper Pairs that created below  $T_c$  and the relation between the density of the Cooper Pairs with the decreasing temperature. These pairs can be seen at figure 2, moving electron inside a conductor attracts protons in the lattice, which results deformation that leads attraction of an electron with an opposite spin to the area with higher proton density. These two electrons are Cooper pairs by the correlation of their. L.P. Gor'kov proved that Ginzburg-Landau equations can be derived from the BCS Theory at near  $T_c$ , in 1959, which we used to understand better the Comsol Simulations [5, 6].

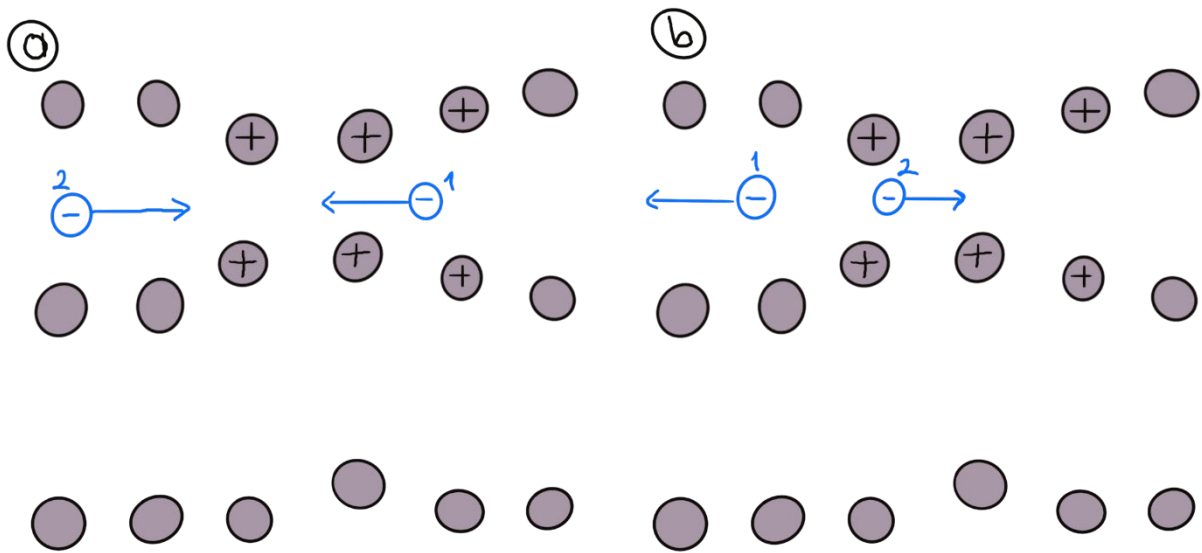


Figure 2 Electron - Phonon interaction where the electron 1 and electron 2 are forming a Cooper Pair

There are two different types of superconductors, Type I and Type II superconductors. Type I superconductors expels the magnetic field completely up to critical magnetic field,  $H_c$ . Type II superconductors behave like a certain point critical magnetic field,  $H_{c1}$ , and for the stronger fields up to critical magnetic field point,  $H_{c2}$ , there is a vortex state. In vortex state superconducting electrons form current vortices hence it allows the material maintain the superconducting properties in the presence of a strong magnetic field.

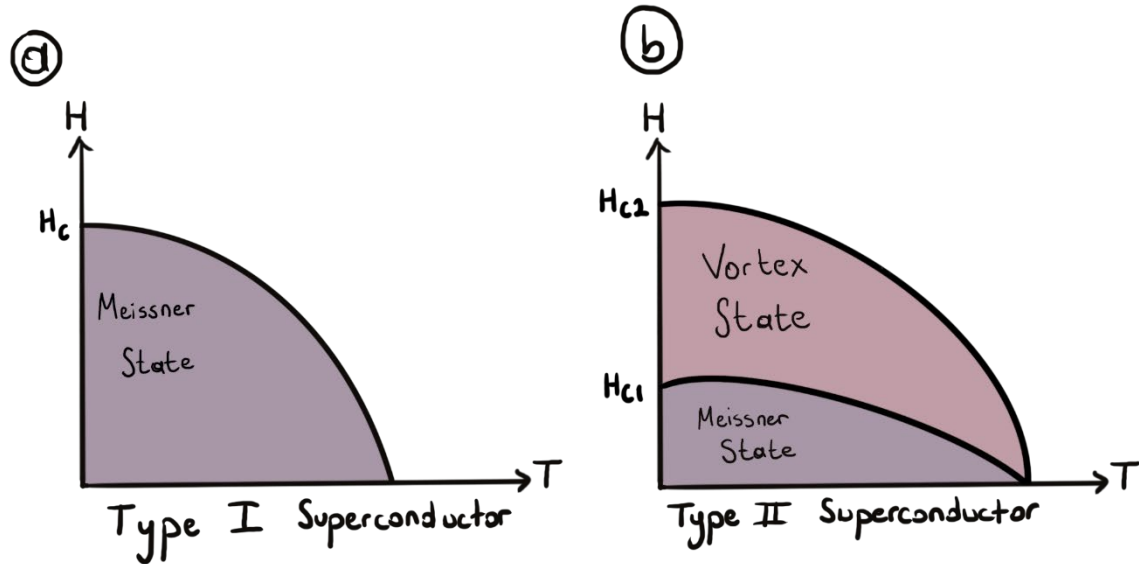


Figure 3  $H$ - $T$  phase diagrams for a) Type I superconductor b) Type II superconductor

## 1.2. The London Brothers' Equations

To explain the experimental results of the Meissner and Ochsenfeld [2], Fritz and Heinz London Brothers proposed a theory that famously known as *Londons' Equations* in 1935 [7]. The equations they proposed are well suited with the electromagnetism and Maxwell's equations, hence when using both superconducting materials and regular materials these equations are great. However, the equations do not satisfy when it is come to explain the quantum and thermodynamics.

As we described superconductor as a *no resistance conductor*, we need to redefine the well-known equations. The resistance  $R$  of a conductor is  $R = \rho L/S$  where  $L$  is length,  $S$  is cross section and  $\rho$  is the resistivity. As  $\rho$  depends on the temperature,  $T$ ,  $\rho(T)$  increase with rising  $T$  in metals and in semiconductors  $\rho(T)$  increase with descending  $T$ . In superconductors  $R = 0$ , hence  $\rho = 0$ . Thus, when working with the Ohm's Law, it makes a lot of problems. In microscopic scale, the Ohm's Law is as follows:

$$j = \sigma E \quad (1.1)$$

where  $j$  is the current density,  $E$  is electric field and  $\sigma$  is the conductivity. As  $\rho = 1 / \sigma = 0$  for superconductors, we conclude that  $\sigma = \infty$ . So, for the infinite current density, the equation 1.1 must be replaced. London Brothers' Approach will guide on that.

If an electric field  $E$  applied to a metal, electron drift occurs. The motion for an electron of this viscous motion is as follows:

$$\ddot{x} = eE/m - \gamma\dot{x} \quad (2.2)$$

where  $m$  is the electron mass,  $e$  is charge,  $\gamma$  is damping coefficient,  $x$  is the coordinate in 1D. The stationary drift velocity is proportional to the acting force:

$$\dot{x} = eE/m\gamma \quad (3.3)$$

So, the electric current density can be written as:

$$j = en\dot{x} = \frac{e^2 n}{\gamma m} E \quad (4.4)$$

where  $n$  is the number of electrons per unit volume. For the conductivity, as applied equations 1.1 and 1.4:

$$\sigma = ne^2\tau/m \quad (5.5)$$

where  $\tau = 1/\gamma$  is the damping time for the motion of electrons. In superconductors, there is no damping. Hence:

$$\sigma|_{\tau \rightarrow \infty} = \infty \quad (6.6)$$

And the equation 1.2 becomes:

$$\ddot{x} = eE/m \quad (7.7)$$

So we can call that equation 1.7 is a Newtonian Motion and the acceleration is proportional to the acting force. To express  $E$  detailly, we define potentials  $A$  and  $\phi$  as follows:

$$E = -\frac{1}{C}\dot{A} - \nabla\phi \quad (8.8)$$

If we say  $\phi$  is scalar and substitute equation 1.8 to 1.2, and integrate as no motion if no field:

$$\dot{\mathbf{x}} = -e\mathbf{A}/mc \quad (9.9)$$

$$\mathbf{j} = e\mathbf{n}\dot{\mathbf{x}} = \frac{-e^2 n}{mc} \mathbf{A} \quad (10.10)$$

Equations 1.9 and 1.10 are Londons' Equations. However, they originally noted these equations as taking the time derivative of equation 1.9 with dropped scalar potential at equation 1.10; and taking the curl of equation 1.10, the original Londons' Equations become:

$$\mathbf{j} = \frac{e^2 n}{m} \mathbf{E} \quad (11.11)$$

$$\text{curl } \mathbf{v} = \frac{-e}{mc} \mathbf{B} \quad (12.12)$$

Equations 1.11 and 1.12 are Londons' Equations and they take an important place as they are Ohm's Law for superconductors. The idea was to assume that the time between scattering of two electrons diverges instead of conductivity is infinite. Hence, they proposed  $\lambda_L$ , The London Penetration Deep, which is the distance that how far a magnetic field penetrates into a superconductor[6]. Which relates to:

$$\mathbf{E} = \frac{\partial}{\partial t} (\Lambda \mathbf{J}); \Lambda = \mu_0 \lambda_L^2 \quad (13.13)$$

### 1.3. The Ginzburg – Landau Equations

As mentioned at chapter 1.2, Londons' Equations fails at describing quantum and thermodynamics. Vitaly Lazarevich Ginzburg and Lev Landau saw that problem and proposed a new theory in 1950 to fill the hole for explaining the superconductivity on thermodynamic manners[8]. With the aid of Landau's earlier works on second order phase transitions, they concluded that a superconductor's Gibbs Free Energy is near to the critical temperature  $T_c$  and can be expressed as a complex parameter  $\psi$  that is the how deep into the distance of the superconducting state is. With minimizing the Gibbs energy respect to  $\psi$  and  $\mathbf{A}$ , Ginzburg and Landau Equations appear as[6]:

$$\alpha\Psi + \beta|\Psi|^2\Psi + \frac{1}{2m}\left(\frac{h}{i}\nabla - qA\right)^2\Psi = 0 \quad (14.14)$$

$$J = \frac{q}{m} \operatorname{Re} \left[ \Psi^* \left( \frac{h}{i} \nabla - qA \right) \Psi \right] \quad (15.15)$$

For simulations that showing a change with time, we need a time dependent Ginzburg – Landau (TDGL) theory. As going to be described in the Josephson Effects, superconductors are described as quantum wave functions,  $\psi$ . The quantum part for the superconductors is the non-dissipative current carrying electrons., also known as Cooper-pair condensate. All conductivity electrons are paired only at absolute zero temperature where  $T = 0$ . At other temperatures, unpaired electrons are also exist. Hence, the current has two parts; non-dissipative part which is quantum mechanical and dissipative part which is classical:

$$\begin{aligned} J &= -(2A - \nabla\theta)|\psi|^2 \text{(non-dissipative)} \\ &\quad + \sigma \left( \frac{\partial A}{\partial t} + \nabla\varphi \right) \text{(dissipative current)} \end{aligned} \quad (16.16)$$

Because of the Coulomb Interaction, non-dissipative and dissipative motions interact. By solving the Schrödinger Equation, the gapless form of the TDGL equation becomes:

$$\begin{aligned} \frac{-\pi}{8T_c} \left( \frac{\partial}{\partial t} + 2i\varphi \right) \Psi + \frac{\pi}{8T_c} [D(\nabla - 2iA)^2] \Psi \\ + \left[ \frac{T_c - T}{T_c} - \frac{7\zeta(3)}{8(\pi T_c)^2} |\Psi|^2 \right] \Psi = 0 \end{aligned} \quad (17.17)$$

Where  $\zeta(3)$  is the Riemann zeta function, D is the diffusion coefficient and  $T_c$  is the critical temperature. The one can find the steps between equation 1.16 and 1.17 at the Shortcut to Superconductivity by Armen Gulian, chapter 2[9].

## 1.4. Harmonic Oscillator

To examine a quantum system, let's begin with the simplest one, quantum harmonic oscillator which described with the Hamiltonian:

$$\hat{H}_{ho} = \frac{\hat{p}^2}{2m} + \frac{1}{2}m\omega^2\hat{x} \quad (18.18)$$

where mass is  $m$ ,  $\omega$  is resonance frequency,  $\hat{p}$  and  $\hat{x}$  are quantum operators for momentum and position. To implement a circuit into a harmonic oscillator, LC circuit is the most basic one where only a capacitor and inductor needed. The total energy stored can be described with the following Hamiltonian:

$$H_{LC} = \frac{CV^2}{2} + \frac{LI^2}{2} = \frac{Q^2}{2C} + \frac{\Phi^2}{2L} \quad (19.19)$$

where  $C$  is the capacitance,  $L$  is the inductance,  $V$  is voltage and  $I$  is the current.  $Q$  defined as  $Q = \int I(t) dt = CV$  and the flux is defined as  $\Phi = \int V(t) dt = LI$ . As  $Q$  and  $\Phi$  are canonical conjugate variables, quantization of the equation 1.19 results quantum Hamiltonian of the LC circuit as follows:

$$\hat{H}_{LC} = \frac{\hat{Q}^2}{2C} + \frac{\hat{\Phi}^2}{2L} \quad (20.20)$$

where  $Q$  and  $\Phi$  are obeys the cummutation rule as  $[\hat{\Phi}, \hat{Q}] = i\hbar$

### 1.4.1. Lumped – Element LC Resonator

A typical circuit quantum electrodynamics experiment consists of LC resonators which are fabricated by a superconducting thin film such as niobium or aluminum on the clean substrate such as silicon. Later, a metal pad shunt into the ground and patterned which constituted a capacitor with the capacitance  $C$  to the ground.  $C$  and inductance defined by the geometry and shape of the metal pad and inductor and typically their range are 1 to 10 GHz frequency and 20 to 200 Ohms impedance [10, 11].

### 1.4.2. $\lambda / 4$ Resonator

As another alternative, from distributive electrical components microwave resonators can be build. A transmission line with short circuit on one end and other end with an open circuit make standing waves with a current node on short end and voltage node on the other end. This type of resonators are named  $\lambda / 4$  resonators. The fundamental mode of this resonator is:

$$\omega_0 = \frac{\pi v_p}{2l} \quad (21.21)$$

where  $l$  is the length of the transmission line,  $v_p$  is the phase velocity. The reason these resonators are called  $\lambda / 4$  is that the fundamental mode supports a standing wave which the transmission line is the  $\frac{1}{4}$  of it's wavelength. The harmonic modes are:

$$\omega_k = (2k + 1)\omega_0, k \in \mathbb{N} \quad (22.22)$$

At the first order, these type of resonators are can be approximated quite close to the resonance frequency with the following parameters[12]:

$$C_k = \frac{\pi}{4Z_0\omega_0} \quad (23.23)$$

$$L_k = \frac{Z_0}{\omega_0} \frac{4}{\pi(2k + 1)^2} \quad (24.24)$$

$$Z_{r,k} = Z_0 \frac{4}{(2k + 1)\pi} \quad (25.25)$$

where  $Z_0$  is the impedance of the transmission line.

### 1.4.3. External Coupling

One more important step is to control the parameters of the resonator made, which can be done with coupling resonator to a drive port. The parameters and impedance, resonance frequency, output coupling rate and quality factor calculations are made with Comsol Multiphysics without defining them. Hence, the derivations of these formulas are

not present here. However, one can find the detailed explanations and derivations [13, 14,15]

### 1.5. Josephson Junctions

Josephson junction depends on a quantum mechanical phenomenon called Josephson effect that flow of the Cooper pairs of electrons through the insulating layer from one superconductor to another with no resistance applied and observed first by Brian Josephson in 1962 which earned him Nobel Prize in Physics in 1973[16].

Josephson junction consists of two superconducting material with separated by a thin layer. Wave like nature of the electrons result a tunneling effect of supercurrent between superconductors through the insulating thin layer with the Josephson relation as follows:

$$I = I_0 \sin\left(\frac{\Phi}{\Phi_0}\right) \quad (26.26)$$

where  $\Phi_0 = \hbar/2e$  is the flux,  $I_0$  is the critical current which is the maximum current can flow through the junction until it keeps the superconducting properties. If we integrate equation 1.26, the potential energy of the Josephson junction becomes:

$$U(\Phi) = -I_0 \Phi_0 \cos\left(\frac{\Phi}{\Phi_0}\right) = -E_j \cos(\varphi) \quad (27.27)$$

Where  $\varphi = \frac{\Phi}{\Phi_0}$  is the dimensionless flux and  $E_j = I_0 \Phi_0$  is the Josephson energy. This energy decreases with the thin insulating layer's thickness. With the help of Ambegaokar-Baratoff's formula, Josephson energy can be easily estimated [17]:

$$E_j = \frac{\Phi_0 \pi \Delta}{2eR_n} \quad (28.28)$$

where  $R_n$  is the junction's resistance at room temperature,  $e$  is electron charge and  $\Delta$  is the superconducting gap of the superconductor.

## 1.6. SQUIDs

SQUID devices, also known as Superconducting Quantum Interference Devices, are highly sensitive electronic devices based on superconductivity and quantum mechanics that used for measuring the extremely small magnetic fields as small as a few picotesla,  $10^{-12}$  T. SQUIDs built by two parallel Josephson Junctions, which aid us to tune the Josephson energy. Let's consider the potential energy of a SQUID:

$$U_{SQUID} = -E_{j,1} \cos \varphi_1 - E_{j,2} \cos \varphi_2 \quad (29.29)$$

As the two of these junctions creates a loop, Faraday's law states that phase drops across the junctions:

$$\Phi_{ext}/\Phi_0 = \varphi_2 - \varphi_1 \quad (30.30)$$

where  $\Phi_{ext}$  is the external magnetic flux. If we rewrite the equation 1.29 by using equation 1.30:

$$\begin{aligned} U_S(\varphi) \\ = -E_\Sigma \sqrt{d^2 + (1 - d^2) \cos^2 \left( \frac{\Phi_{ext}}{2\Phi_0} \right)} \cos(\varphi) \end{aligned} \quad (31.31)$$

where  $E_\Sigma = E_{j,1} + E_{j,2}$ , is the total junction energy,  $d = \frac{(E_{j,1} - E_{j,2})}{E_\Sigma}$  is the SQUID asymmetry, and  $\varphi = \left( \frac{\varphi_1 + \varphi_2}{2} \right) - \arctan(d \tan(\Phi_{ext}/2\Phi_0))$  [18]. As we compare equation 1.31 with equation 1.27, we see that SQUID loop is behaves like a single Josephson junction.

## 1.7. The Transmon Qubit

There are lots of different types of qubits: superconducting qubits, photonic qubits, trapped ion qubits, topological qubits, spin qubits and quantum dot qubits. At this thesis, we aim on superconducting qubits. Superconducting qubits are also separate into 5 different types: transmon qubits, xmon qubits, flux qubits, phase qubits and hybrid qubits. Our interest is in transmon qubits while they are based on the superconducting Josephson Junctions. Also, it is relatively easy to fabricate and control, which makes it a highly demanding choice for quantum computing, compared to other types.

The transmon qubit is based on two superconductors named island and reservoir that connected by Josephson Junctions to form SQUID. Hamiltonian of this system is:

$$\hat{H} = 4E_c(\hat{n} - n_g)^2 - E_J \cos \hat{\phi} \quad (32.32)$$

where  $\hat{n}$  number of Cooper pairs,  $\hat{\phi}$  is the phase difference between two superconductors.

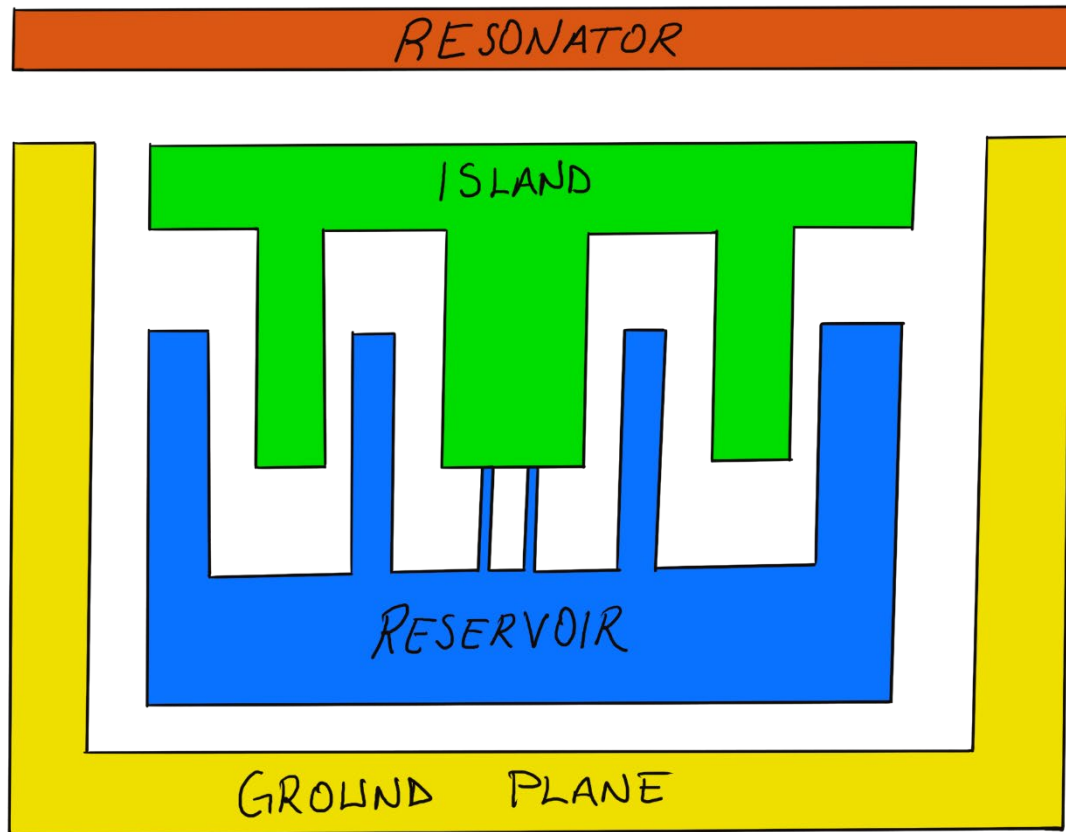


*Figure 4 Schematic of transmon qubit, superconducting island and reservoir by josephson junctions. Resonator is coplanar waveguide resonator.*

### 1.8. Jaynes – Cummings Hamiltonian For Qubit – Resonator Couple

The Jaynes – Cummings Hamiltonian is a theoretical model proposed by Edwin T. Jaynes and Frederick W. Cummings in 1963 to explain the interaction between two-level atom and electromagnetic field mode in a cavity [19].

To investigate the transmon qubit and use it functionally, we need to readout and manipulate the state of our qubit. For the readout of the state, coplanar waveguide resonator (CPW) placed close to the qubit. Hence the transmon qubit is coupled to the cpw resonator. The Hamiltonian of the system can be explained with the aid of Jaynes-Cummings Model as follows:

$$\hat{H} = \hbar \sum_i w_i |i\rangle\langle i| + \hbar\omega_r a^\dagger a + \hbar \sum_{i,j} g_{ij} |i\rangle\langle j| (a + a^\dagger) \quad (33.33)$$

Where the first term of the equation describing the transmon, and the second term describing the resonator.  $|i\rangle$  is energy eigenstate,  $\hbar w$  is the energy.  $a$  and  $a^\dagger$  are annihilation and creation operators for the excitations of the resonator. And the third term here, describes the qubit's and resonator's interaction[20]. Where the couplings is:

$$g_{ij} = \frac{2e}{\hbar} \frac{C_g}{C_\Sigma} \sqrt{\frac{\hbar\omega_r}{2C_r}} \langle i | n | j \rangle \quad (34.34)$$

Where  $C_r = \pi/(2w_r Z_0)$ . By using the RWA (rotating wave approximation) and noticing just first two lowest transmon levels, the Jaymes-Cummings Hamiltonian becomes:

$$\hat{H} = -\frac{\hbar w_q}{2} \sigma_z + \hbar\omega_r \left( a^\dagger a + \frac{1}{2} \right) + \hbar g (a^\dagger \sigma^- + a \sigma^+) \quad (35.35)$$

## 2. COMPUTATIONAL

### 2.1. Superconducting Disk In a Magnetic Field with London Brother's Approach

For the first investigation of the expulsion of a magnetic field, it is easy to start with stationary conditions. For stationary conditions, London Brother's approach is suitable.

For the stationary conditions, Maxwell Equations for the case of magnetostatics are:

$$\nabla \cdot \mathbf{B} = \mathbf{0} \quad (2.1)$$

$$\nabla \times \mathbf{B} = 4\pi \mathbf{j} \quad (2.2)$$

$$\mathbf{B} = \nabla \times \mathbf{A} \quad (2.3)$$

Where  $\mathbf{B}$  is magnetic field and  $\mathbf{j}$  is the current density. By substituting equation 2.3 into equation 2.2, we get:

$$\nabla \times (\nabla \times \mathbf{A}) = \nabla(\nabla \cdot \mathbf{A}) - \nabla^2 \mathbf{A} = 4\pi \mathbf{j} \quad (2.4)$$

As choosing the “London Gauge” which is  $\text{div} \mathbf{A} = 0$ , and substituting equation 1.10 into equation 2.4, one can get:

$$\nabla^2 \mathbf{A} = \frac{1}{\lambda_L^2} \mathbf{A} \quad (2.5)$$

Where the  $\lambda_L$  is the London Penetration Length. Here,  $\mathbf{j} \propto -\mathbf{A}$ , hence:

$$\nabla^2 \mathbf{j} = \frac{1}{\lambda_L^2} \mathbf{j} \quad (2.6)$$

$$\nabla^2 \mathbf{B} = \frac{1}{\lambda_L^2} \mathbf{B} \quad (2.7)$$

As the gauge can be non-zero just in superconductors, equation 2.5 may also be written as:

$$\nabla^2 \mathbf{A} = \frac{\mathbf{I}(\mathbf{r})}{\lambda_L^2} \mathbf{A} \quad (2.8)$$

Where inside a superdoctor  $\mathbf{I}(\mathbf{r})$  is 1 and 0 at outside. The external magnetic field is homogeneous and perpendicular to the surface of the disk. As the disk defined at cylindrical coordinates,  $\mathbf{A}$  depends only on coordinates  $(r,z)$ . Hence, the equation 2.8 becomes:

$$\nabla^2 \mathbf{A} = \frac{\mathbf{I}(r, z)}{\lambda_L^2} \mathbf{A} \quad (2.9)$$

If one know the scalar  $A$ , magnetic induction calculated with:

$$\mathbf{B} = \nabla \times \mathbf{A} = -\frac{\partial A}{\partial z} \hat{\mathbf{r}} + \frac{1}{r} \frac{\partial(rA)}{\partial r} \hat{\mathbf{z}} \quad (2.10)$$

By defining the necessary variables and solving the equation 2.10 PDE on comsol, one can simulate the superconducting disk in a magnetic field with London Brothers' Approach.

Parameters		
Name	Expression	Value
r0	10[mm]	0.01 m
h0	2[mm]	0.002 m
R0	20[mm]	0.02 m
H0	20[mm]	0.02 m
B0	1[T]	1 T
LL	0.16[mm]	1.6E-4 m

Figure 5 Disk in a magnetic field with London Brothers' Approach parameters at COMSOL Multiphysics interface

As can be seen at figure 5, the parameters of  $r_0$ ,  $h_0$ ,  $R_0$ ,  $H_0$ ,  $B_0$  and  $LL$  are defined which are respectively superconducting disk radius, superconducting disk height, box radius, box height, magnetic field at infinity and London Penetration Depth.

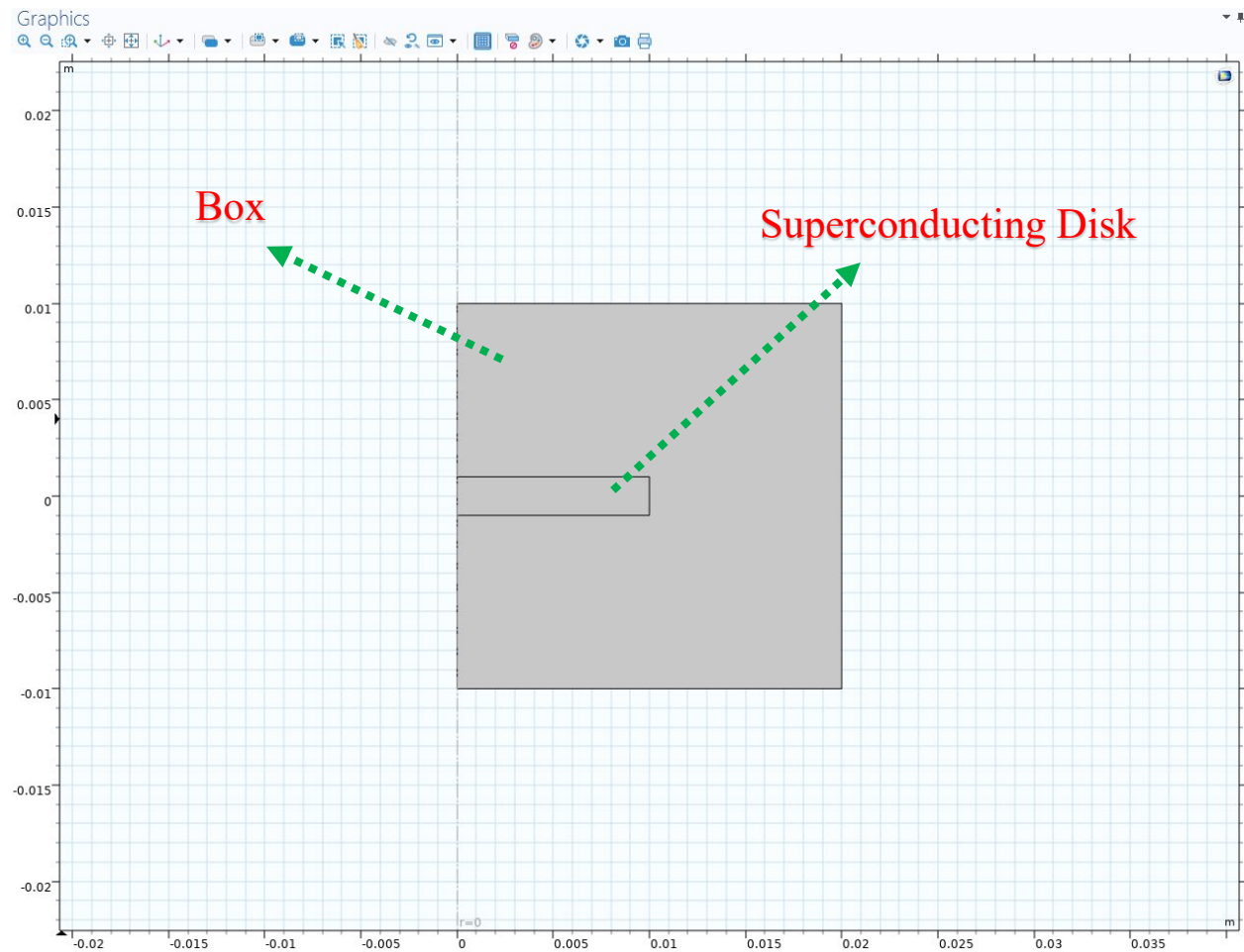


Figure 6 Geometry of Superconducting Disk and the box on COMSOL Multiphysics GUI

The disk centered at the position  $z = -h_0/2$  and  $z = -H_0/2$  for them to be symmetrically relative to y-axis.

**Coefficient Form PDE**

Label: Coefficient Form PDE 1

Domain Selection

Override and Contribution

**Equation**

Show equation assuming:  
Study 1, Stationary

$$e_s \frac{\partial^2 u}{\partial t^2} + d_s \frac{\partial u}{\partial t} + \nabla \cdot (-c \nabla u - \alpha u + \gamma) + \beta \cdot \nabla u + \alpha u = f$$

$$\nabla = [\frac{\partial}{\partial r}, \frac{\partial}{\partial z}]$$

**Diffusion Coefficient**  
 $c$ : 1  
Isotropic

**Absorption Coefficient**  
 $\alpha$ :  $(r < r_0)^*(z^2 < h_0^2/4)/LL^2$   $1/m^2$

**Source Term**  
 $f$ : 0  $1/m^2$

**Mass Coefficient**  
 $e_a$ : 0  $s^2/m^2$

**Damping or Mass Coefficient**  
 $d_a$ : 0  $s/m^2$

Conservative Flux Convection Coefficient

Convection Coefficient

Conservative Flux Source

Figure 7 Coefficients From PDE defined as shown on COMSOL Multiphysics for the case of superconducting disk on a magnetic field with London Brothers' approach simulation

By adding mesh and computing the PDE, the simulation can be done.

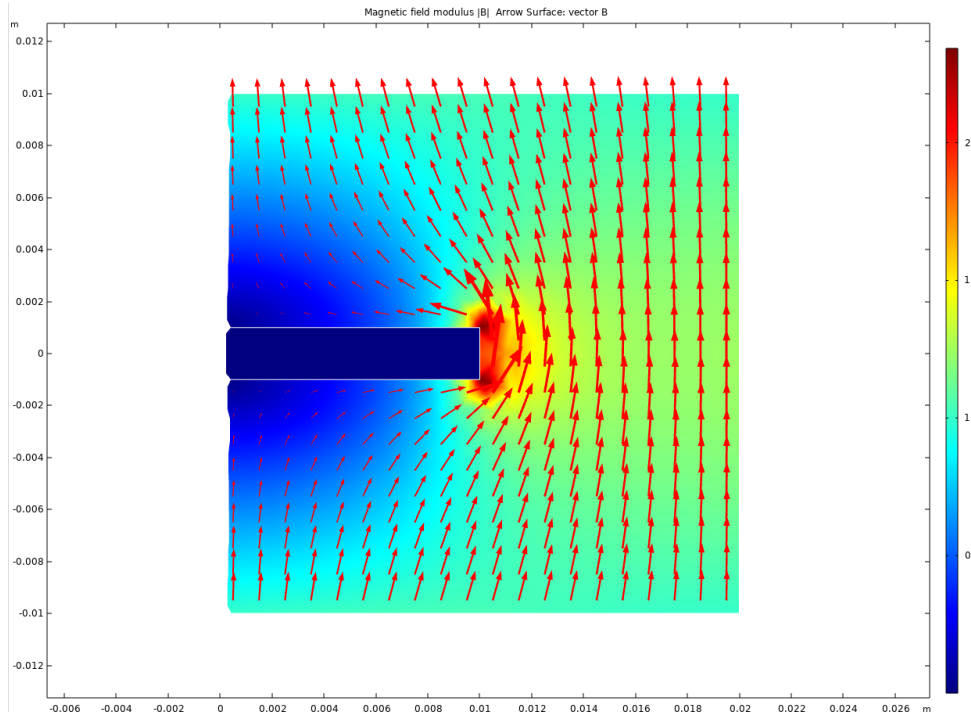


Figure 8 Result of the superconducting disk on a magnetic field with London Brothers' approach simulation

## 2.2. Meissner Effect with Ginzburg – Landau Approach

For this simulation, same problem but with a different approach investigated: disk in a magnetic field with Ginzburg – Landau Approach. We do expect this simulation will result more information relative to London Brothers' Approach. Also, as TDGL is a time dependent theory, we will also investigate the track of the dynamics of this simulation.

▼ Parameters		
Name	Expression	Value
kappa	4	4
sigma	1	1
Ba	0.9	0.9
R	5	5
t0	200	200
delta_t	0.1	0.1

Figure 9 Input Parameters for Meissner Effect with Ginzburg-Landau Approach simulation on COMSOL Multiphysics

As stated in figure 9, the input parameters are kappa, sigma, Ba, R, t0 and delta\_t which are respectively Ginzburg – Landau parameter, the conductivity of normal electrons, external field value, radius of the disk, calculation time and time step.

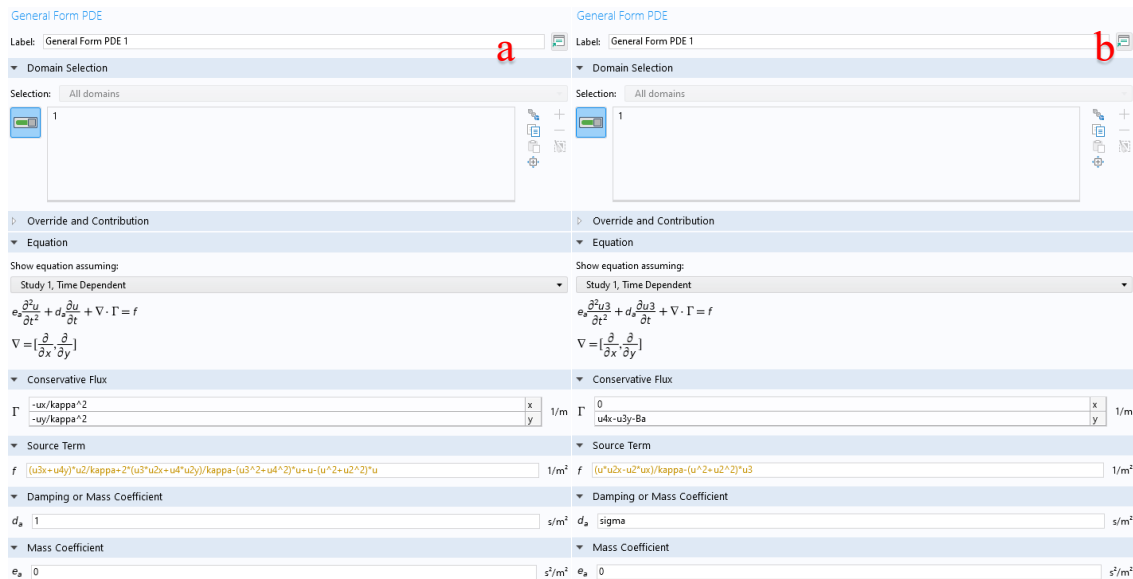


Figure 10 a)Equation for the real part of the wave function where =u, b) Equation for the imaginary part of the wave function

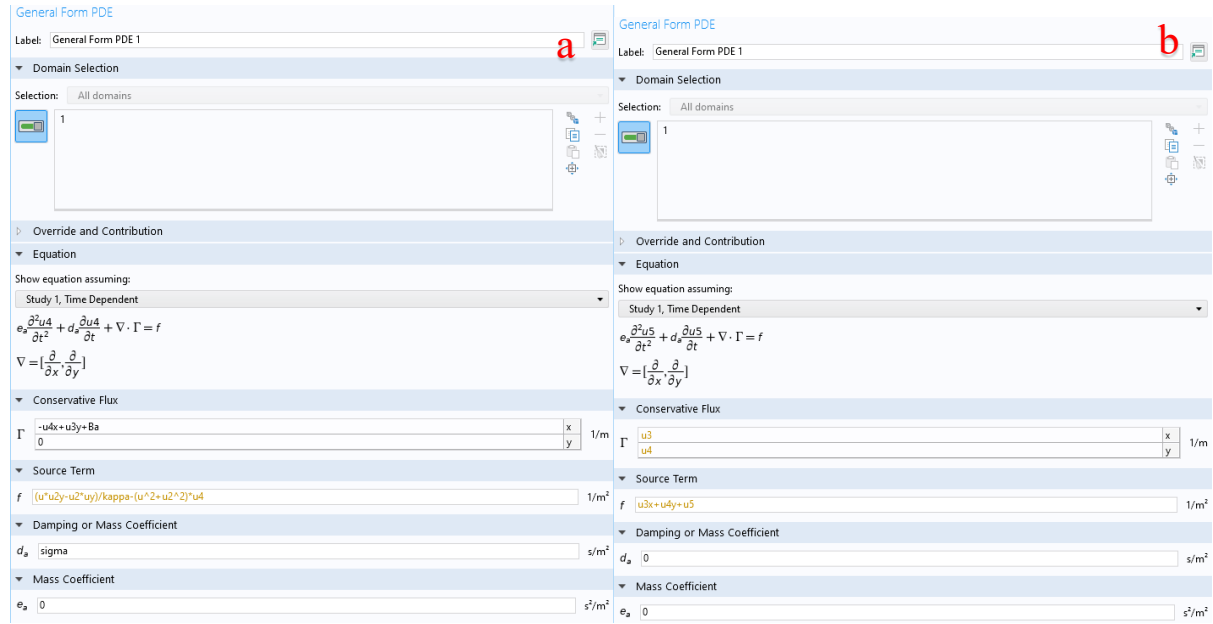


Figure 11 a) Equation for Ax b) Equation for Ay

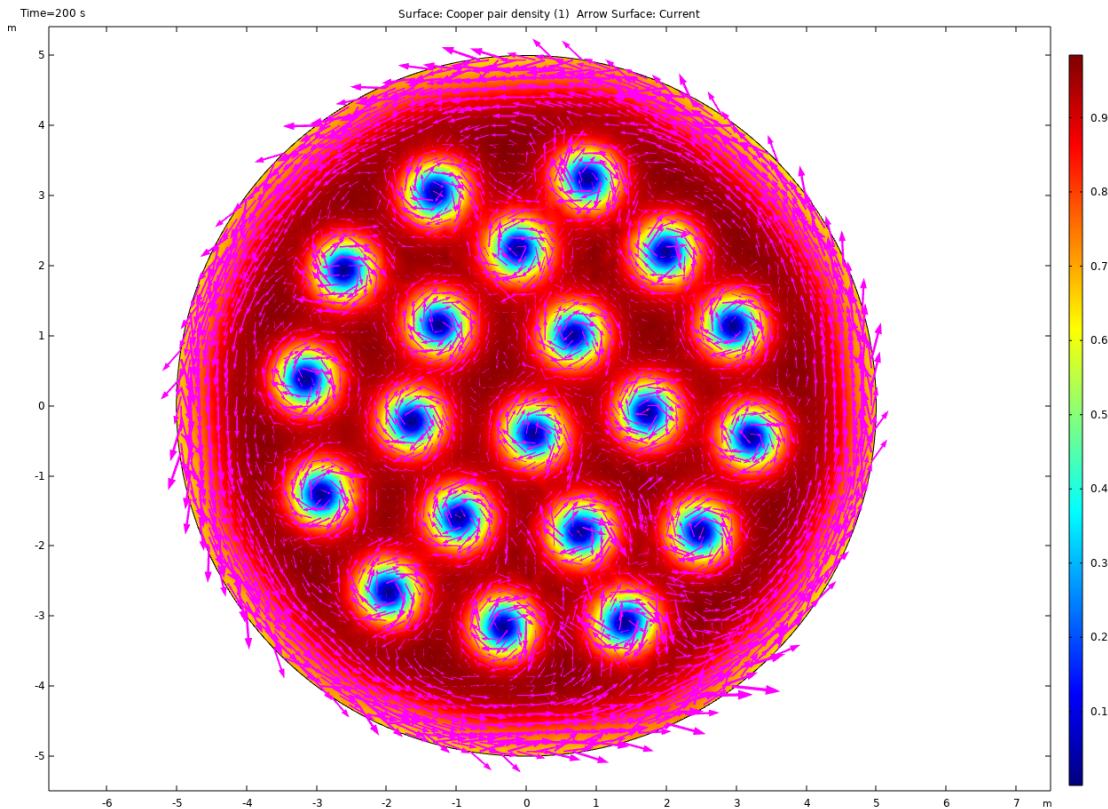


Figure 12 Vortex pattern at  $t=200s$

### 2.3. Meissner Effect with Easier Approach to Boundary Conditions

At section 2.2, the simulation was so straightforward to solve with given standart TDGL equations. On the other hand, we may require different boundary conditions to solve for varying problems. Hence, it is necessary to solve the same Meissner Effect simulation with different boundary conditions.

Let's assume a superconducting object inside a non-superconducting and non-magnetic material with so little conductivity. So, it can be stated that this material has no effect on the superconductor. To solve the TDGL equations, we define that wave function is zero in the non-superconducting material. So the equation becomes:

$$\frac{\partial \psi}{\partial \tau} = vol(x, y, z) \left[ -\left( \frac{i}{\kappa} \nabla + \mathbf{A} \right)^2 + 1 - |\psi|^2 \right] \quad (2.11)$$

Where the  $vol(x, y, z)$  function is:

$$vol(x, y, z) = \begin{cases} 1, & \text{if } (x, y, z) \in \text{superconductor} \\ 0, & \text{otherwise} \end{cases} \quad (2.12)$$

Boundary conditions of the wave function is zero with te Dirichlet Boundary condition. The  $\mathbf{A}$  function is non-zero at everywhere. Superconducting disk with radius  $r$  and with a surrounding object with radius  $R$  created with COMSOL.

Parameters

Label: Parameters 1		
<b>▼ Parameters</b>		
▶ Name	Expression	Value
kappa	4	4
sigma	1	1
Ba	0.9	0.9
R	15	15
r	5	5
t0	200	200
delta_t	0.1	0.1

Figure 13 Parameters are the same as before, but  $R$  and  $r$  are added

As stated in figure 13, the input parameters are kappa, sigma, Ba, R, r, t0 and delta\_t which are respectively Ginzburg – Landau parameter, the conductivity of normal electrons, external field value, radius of the surrounding object, radius of the disk, calculation time and time step.

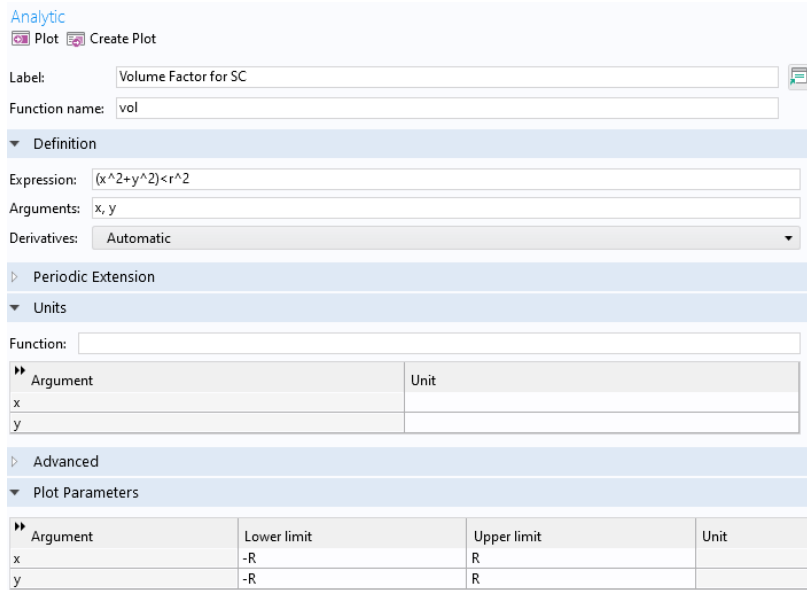


Figure 14 Here the vol function is defined in COMSOL

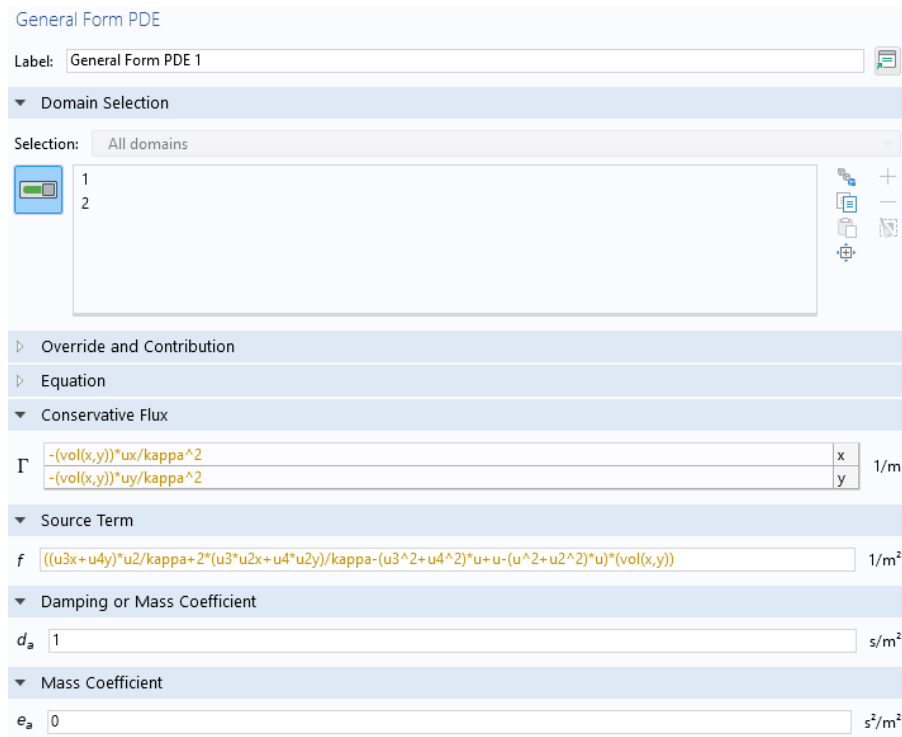


Figure 15 TDGL Equations with vol function inserted in COMSOL GUI

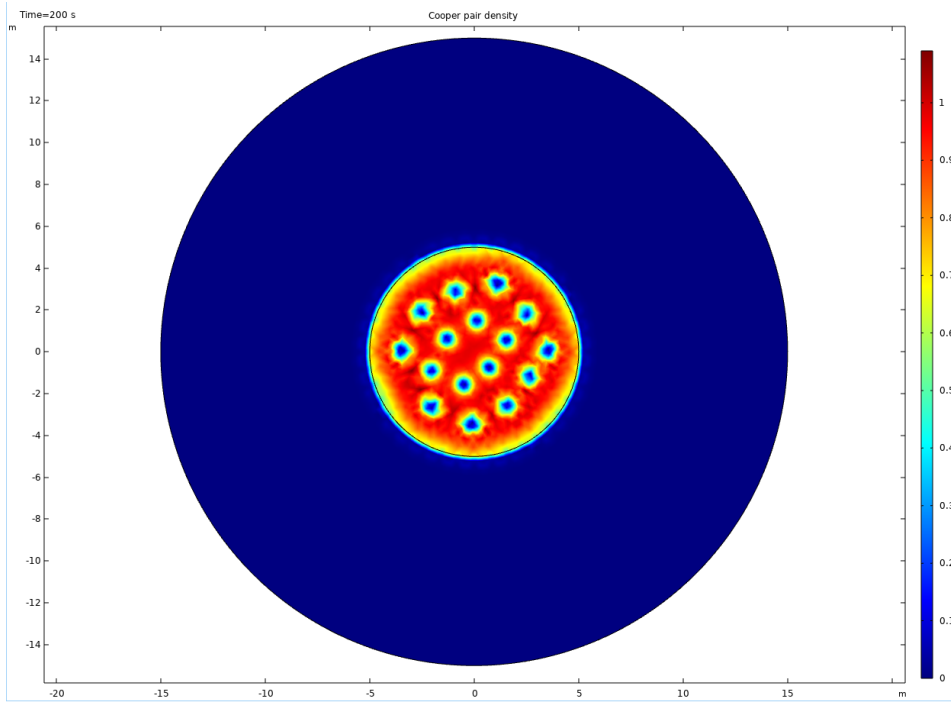


Figure 16 Evolution of vortices for the time at  $t=200s$  on COMSOL GUI

## 2.4. Simulation of Current Carrying Superconducting Wires

This time, let us consider a 1 dimensional wire and their current carrying states. There are phase slips occur in 1 dimensional superconducting wires, which can also be states as crossover from quantum tunneling to thermal hopping[21].

Parameters		
Label: Parameters 1		
▼ Parameters		
» Name	Expression	Value
sigma	1	1
j0	0.4	0.4
L0	10	10
kappa	0.4	0.4
A0	0	0
gamma	0	0
p	-0.3	-0.3
x0	5	5
width	0.1	0.1
t0	100	100
delta_t	0.01	0.01

Figure 17 Parameters for the 1D Superconducting wire in COMSOL GUI

Where sigma is conductivity, j0 is current density, L0 is length of the wire, kappa is Ginzburg – Landau parameter, A0 is AB-potential, gamma is gap value, p is inhomogeneity amplitude, x0 is inhomogeneity position, width is inhomogeneity scale, t0 is evolution time and delta\_t is the time step.

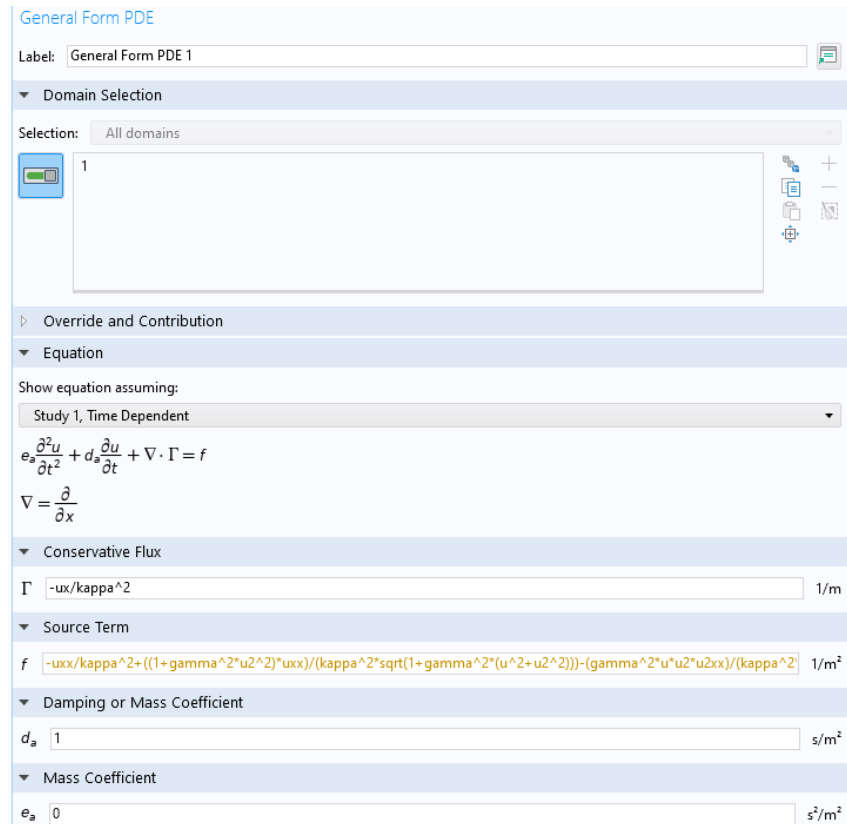


Figure 18 TDGL Equations are written as follows in COMSOL GUI

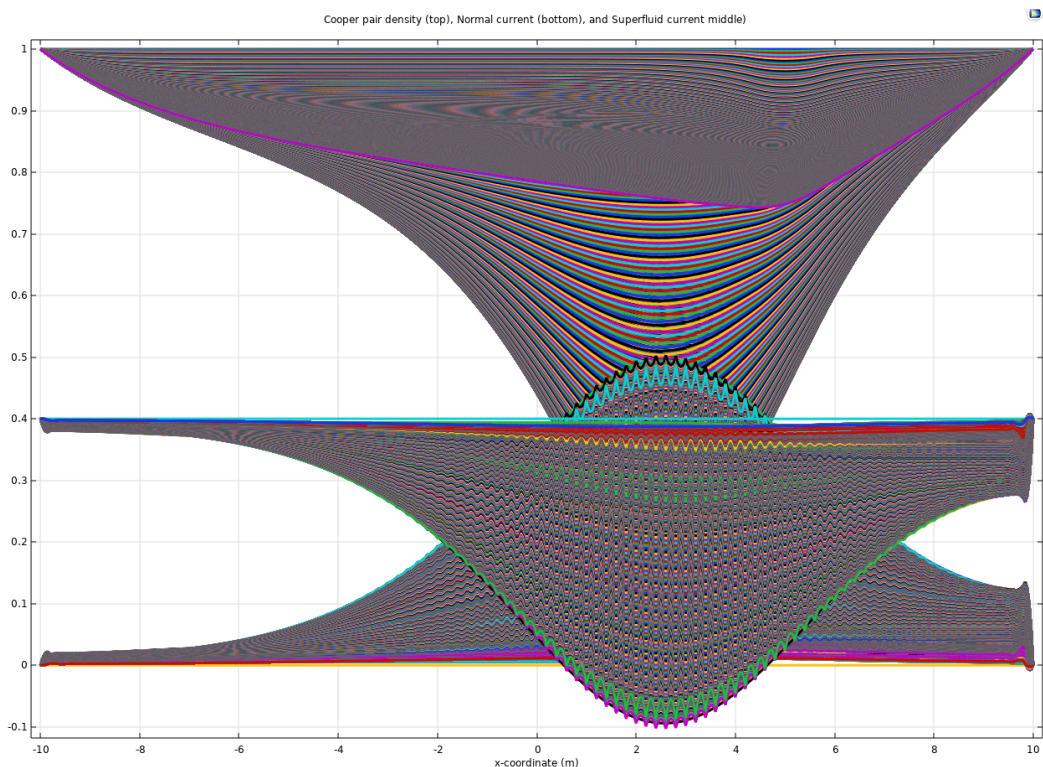


Figure 19 Cooper pair density at top, normal current at bottom and superfluid current at the middle showing that their change with respect to time in COMSOL GUI

## 2.5. Flowing Current in Thin Superconducting Strips

For this simulation, let's take in action a thin film superconductor and flowing of an electric current through it.

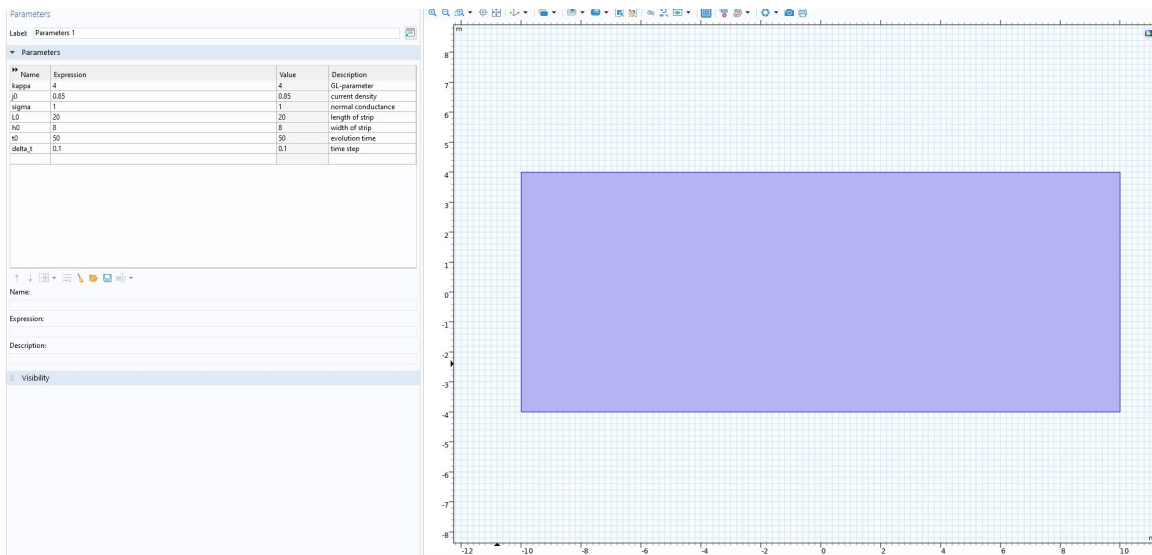


Figure 20 Parameters for the relevant simulation and the 2D geometry of the thin film in COMSOL GUI

General Form PDE

Label: General Form PDE 1

- ▷ Domain Selection
- ▷ Override and Contribution
- ▼ Equation

Show equation assuming:

Study 1, Time Dependent

$$e_a \frac{\partial^2 u}{\partial t^2} + d_a \frac{\partial u}{\partial t} + \nabla \cdot \Gamma = f$$

$$\nabla = \left[ \frac{\partial}{\partial x}, \frac{\partial}{\partial y} \right]$$

- ▼ Conservative Flux

$\Gamma$	$-ux/\kappa^2$	x	1/m
	$-uy/\kappa^2$	y	

- ▼ Source Term

$f$	$(u^3x+u^4y)u^2/\kappa^2 + 2*(u^3*u^2x+u^4*u^2y)/\kappa - (u^3+u^4)^2*u + u - (u^2+u^2)^2*u$	1/m <sup>2</sup>
-----	--	------------------

- ▼ Damping or Mass Coefficient

$d_a$	1	s/m <sup>2</sup>
-------	---	------------------

- ▼ Mass Coefficient

$e_a$	0	s <sup>2</sup> /m <sup>2</sup>
-------	---	--------------------------------

Figure 21 TDGL Equations for Thin Film Superconductivity

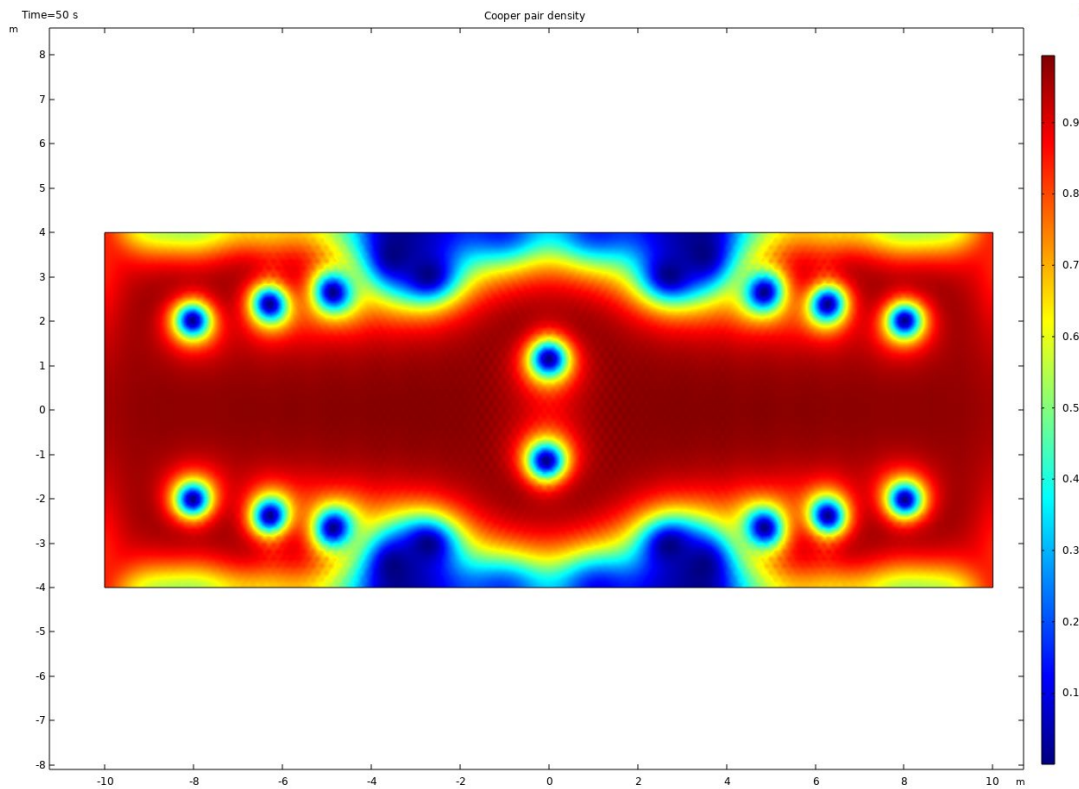


Figure 22 Flow of the electric current in the superconductors cause vortice pattern

## 2.6. Creating Single Flux Quantum Pulses Using COMSOL

Let's consider a Superconductor – Normal Metal – Superconductor (SNS) junction which is similar to Josephson Junction but consisting of two superconductor and a normal metal layer between these two superconductors. Also, instead of a very thin tunnel barrier on Josephson junctions, thicker normal metal layer is used in SNSs.

When a superconductor and a metal get in contact at each other, Cooper pairs propagate. Hence, thin layer of the metal acts like a superconductor, which is called the “proximity effect”.

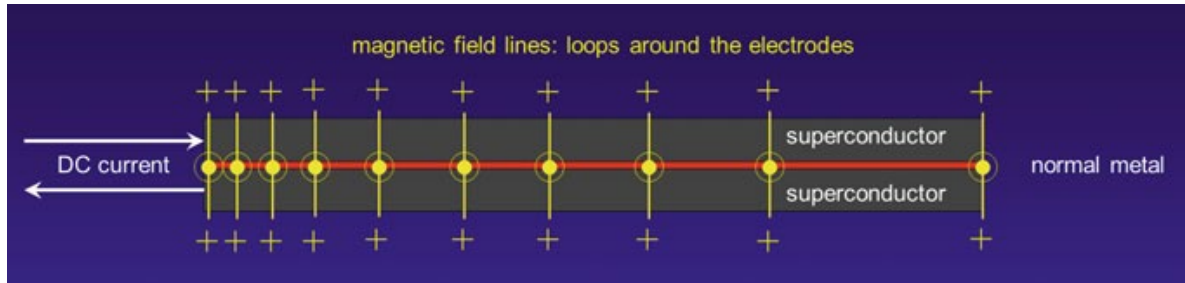


Figure 23 Superconductor-Normal metal-Superconductor junction [9]

### Parameters

Label: Parameters 1

#### ▼ Parameters

Name	Expression	Value
kappa	4	4
L0	5	5
h0	4	4
gamma	0	0
myu	0	0
p	-0.3	-0.3
r0	0.14	0.14
Ba	0.65	0.65
sigma	1	1
t0	100	100

Figure 24 Parameter to create SFQ pulse on SNS junction on COMSOL GUI

Parameters can be seen at figure 24, where kappa is Ginzburg – Landau Parameter, L0 is the length of the metal, h0 is the height, p is the p-function value, r0 is the radius, Ba is the external field value, sigma is the conductivity, t0 is the time evolution.

General Form PDE

Label: General Form PDE 1

▷ Domain Selection

▷ Override and Contribution

▼ Equation

Show equation assuming:

Study 1, Time Dependent

$$e_a \frac{\partial^2 u_2}{\partial t^2} + d_a \frac{\partial u_2}{\partial t} + \nabla \cdot \Gamma = f$$

$$\nabla = \left[ \frac{\partial}{\partial x}, \frac{\partial}{\partial y} \right]$$

▼ Conservative Flux

$$\Gamma = \begin{bmatrix} -u_2 x / \kappa^2 \\ -u_2 y / \kappa^2 \end{bmatrix}$$

1/m

▼ Source Term

$$f = \frac{-(u_{2xx} + u_{2yy}) / \kappa^2 + ((1 + \gamma^2) u^2)^2 (u_{2xx} + u_{2yy})}{(\kappa^2 \sqrt{1 + \gamma^2 u^2}) - (\gamma^2 u^2)} \quad 1/m^2$$

▼ Damping or Mass Coefficient

$$d_a = 1 \quad s/m^2$$

▼ Mass Coefficient

$$e_a = 0 \quad s^2/m^2$$

Figure 25 TDGL Equations of the relevant simulation on the COMSOL GUI

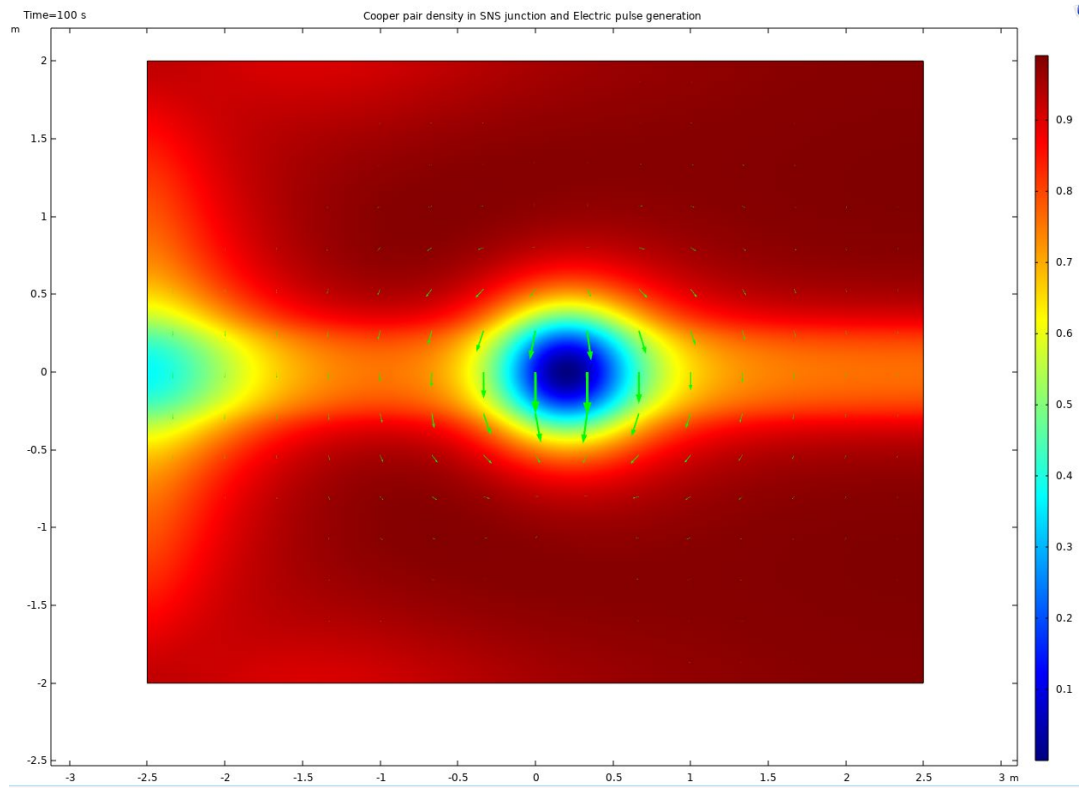


Figure 26 SFQ Generation on SNS junction at time  $t=100s$  in COMSOL GUI

## 2.7. Cloning Single Flux Quantum Pulses using COMSOL

For some of the specific needs, one may require not to create a SFQ pulse but to clone for superconducting electronics. Which is to recreate a SFQ with propagating voltage pulses.

Parameters		
Label: Parameters 1		
▼ Parameters		
► Name	Expression	Value
kappa	4	4
L0	5	5
h0	4	4
gamma	0	0
mymu	0	0
p	-0.3	-0.3
r0	0.14	0.14
Ba	0.45	0.45
sigma	1	1
t0	150	150
t1	20	20
delta_t	5	5

Figure 27 Parameters used

Parameters are all the same with the last parameters used in the section 2.6, however there are 2 other parameters used here: t1 and delta\_t which are arrival time of SFQ and width of the SFQ pulse respectively.

General Form PDE

Label: General Form PDE 1

► Domain Selection

► Override and Contribution

▼ Equation

Show equation assuming:

Study 1, Time Dependent

$$e_s \frac{\partial^2 u}{\partial t^2} + d_s \frac{\partial u}{\partial t} + \nabla \cdot \Gamma = f$$

$$\nabla = [\frac{\partial}{\partial x}, \frac{\partial}{\partial y}]$$

▼ Conservative Flux

$\Gamma$	$-\frac{ux}{kappa^2}$	x	1/m
	$-\frac{uy}{kappa^2}$	y	

▼ Source Term

$f = -\frac{(uxx+uyy)}{kappa^2} + ((1+gamma^2*u2^2)*(uxx+uyy)) / (kappa^2 * sqrt(1+gamma^2*(u^2+u2^2))) - (gamma^2*u*u2*(u2))$  1/m<sup>2</sup>

▼ Damping or Mass Coefficient

$d_a$  1 s/m<sup>2</sup>

▼ Mass Coefficient

$e_a$  0 s<sup>2</sup>/m<sup>2</sup>

Figure 28 TDGL Equations for cloning the SFQ Pulses on COMSOL GUI

## 2.8. Transmon Qubit in a Coplanar Waveguide Cavity

At this simulation, the system is stationary so TDGL equations are not used. Two geometry are defined, one is work plane, which is circuit, and the other is the whole 3D Geometry to work with.

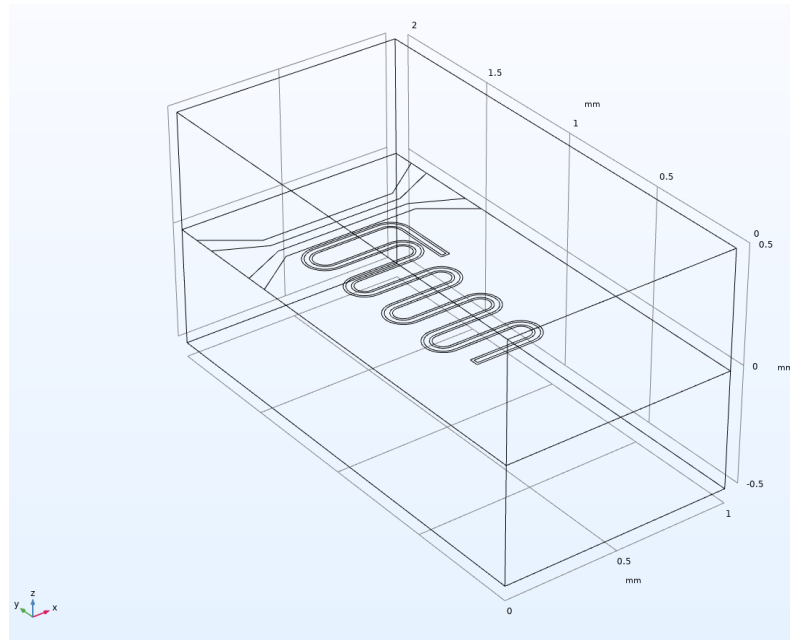


Figure 29 3D Working Geometry in COMSOL GUI

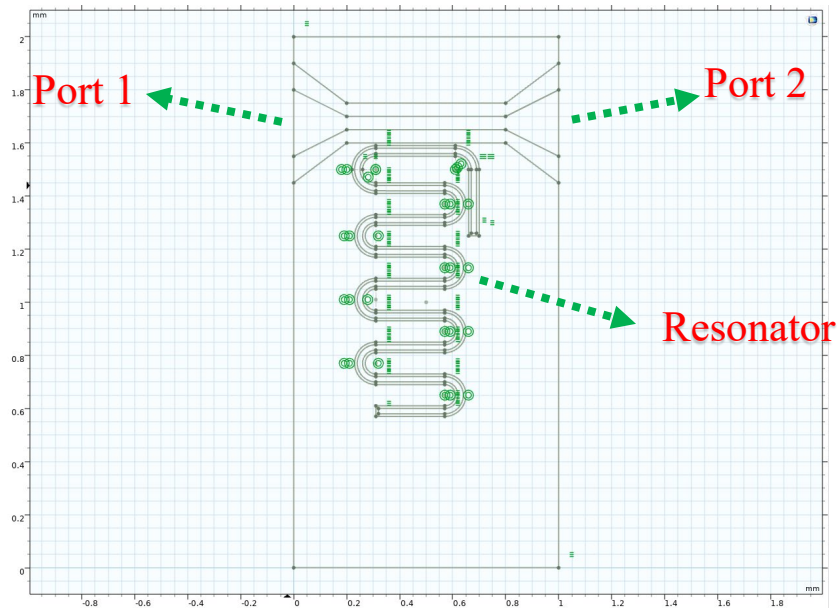


Figure 30 Plane Geometry of the qubit-cavity coupler circuit

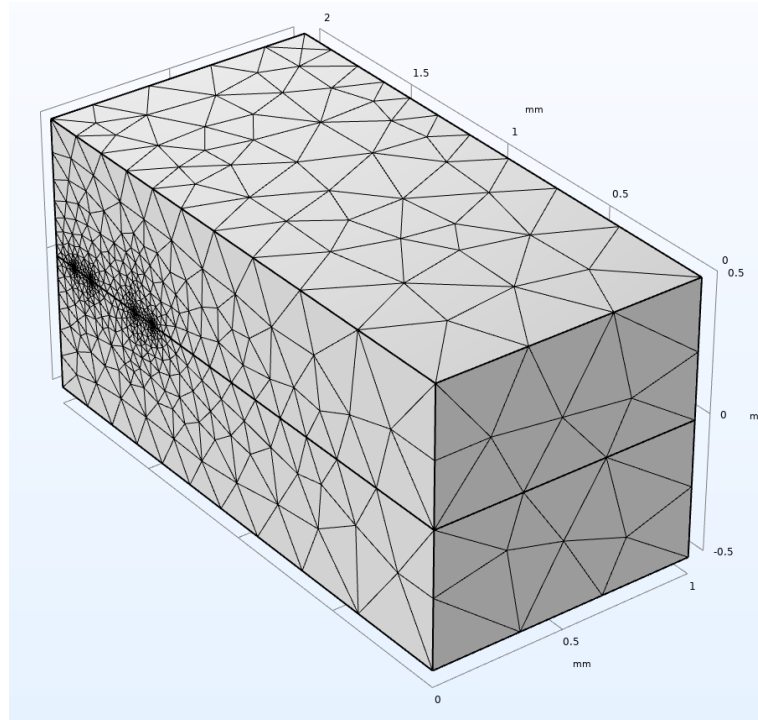


Figure 31 Mesh Geometry

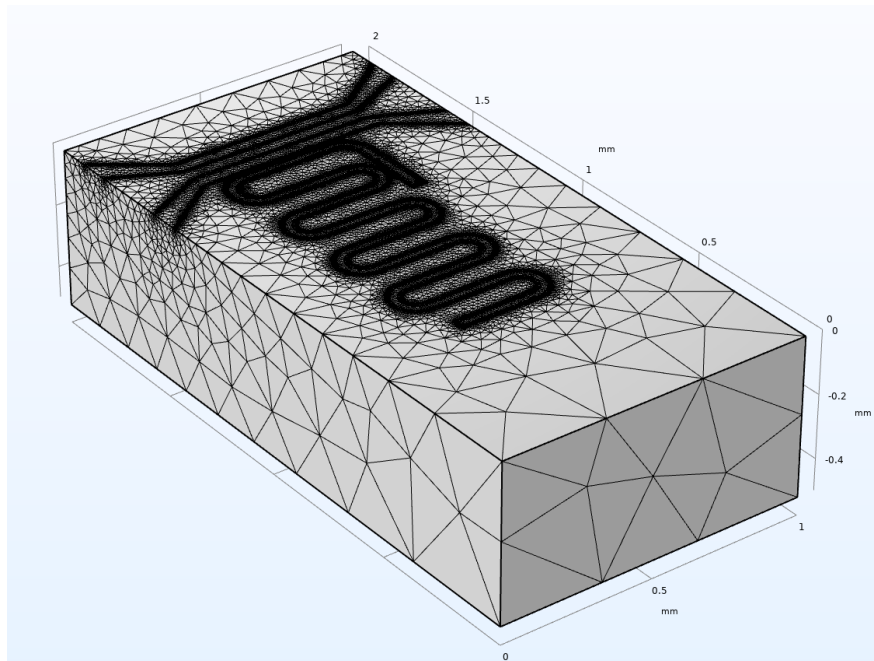


Figure 32 Mesh Geometry showing down part and the cross section between up and down geometries

### 3. RESULTS & DISCUSSION

At the first simulation, we made a superconducting disk in a magnetic field using London Brothers' Approach and investigate its properties.

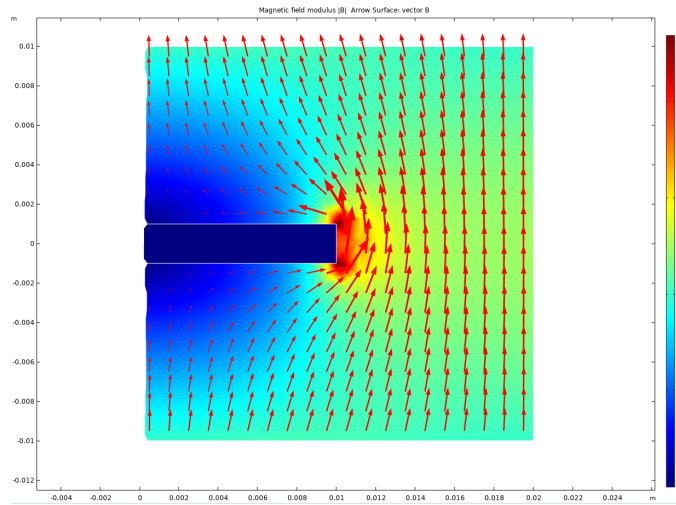


Figure 33 Meissner effect in superconducting disk using London Brothers' Approach

As can be seen at figure 33, the Meissner effect is present and external magnetic field is expelled from the superconducting disk.

For the next simulation, we solve the same problem; superconducting disk in a magnetic field. However, this time we also define Time Dependent Ginzburg – Landau equations to solve it with respect to time.

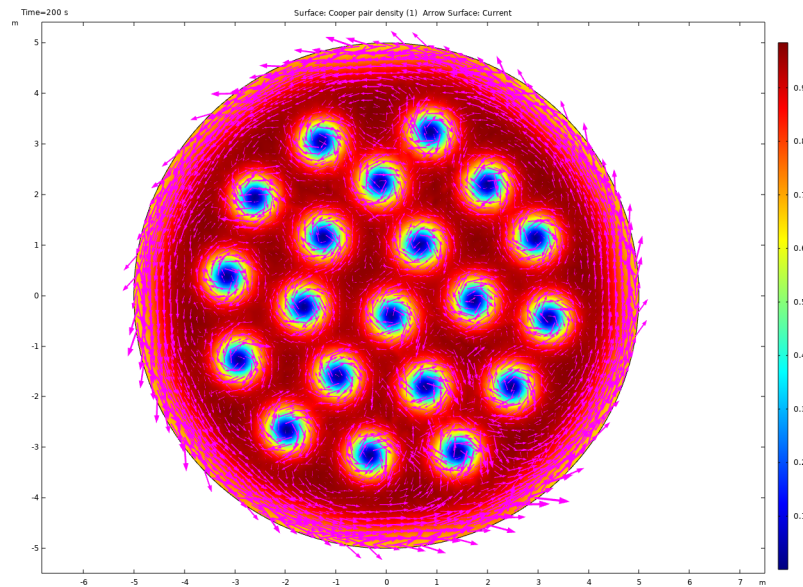


Figure 34 Meissner Effect on Superconducting Disk in a magnetic field using TDGL equations

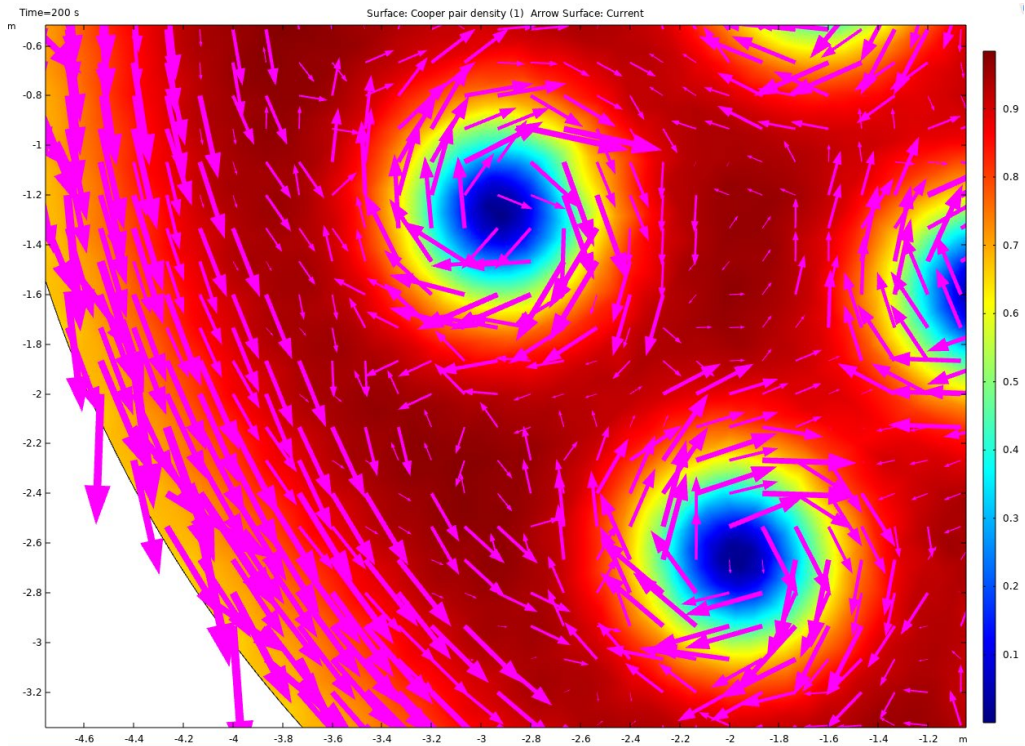


Figure 35 Close - up of the figure 34

As can be seen from from the figure 35, current density vectors have opposite rotational direction. Also, this final formation shows the state at time  $t=200\text{s}$ . This formation build can be seen step by step with the following figure 36.

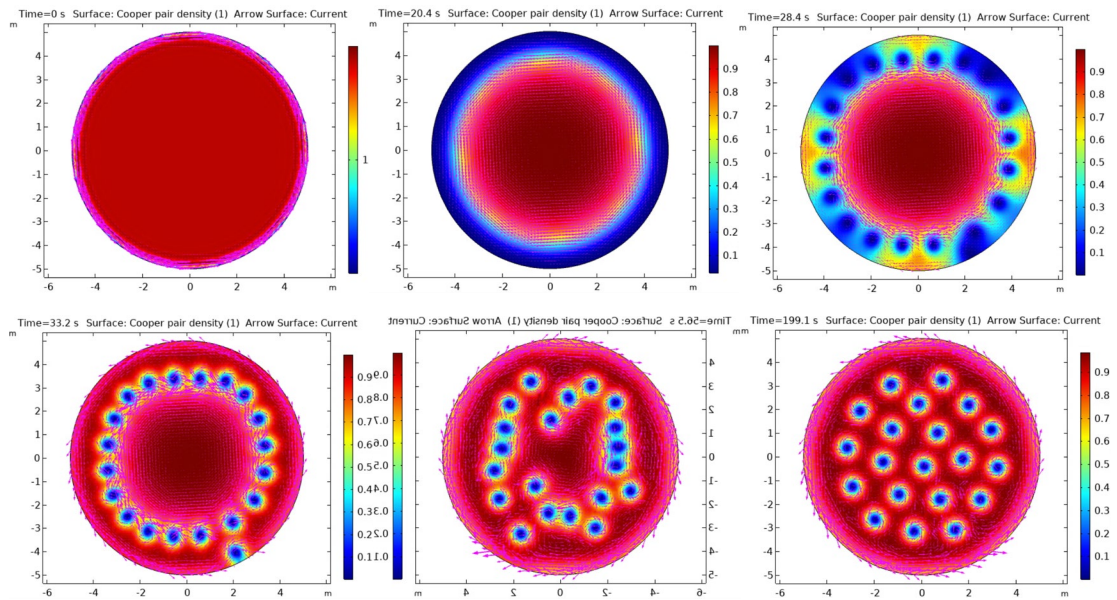


Figure 36 Formation of the simulation of Meissner Effect using TDGL Equations where showing the time at  $t=0, 20.4\text{s}, 28.4\text{s}, 33.2\text{s}, 51.3\text{s}$  and  $120\text{s}$

For the next simulation, same problem as before investigated but this time the boundary conditions are changed. Evolution of the vortices from time  $t=0$  to  $t=200$ s can be seen at figure 37.

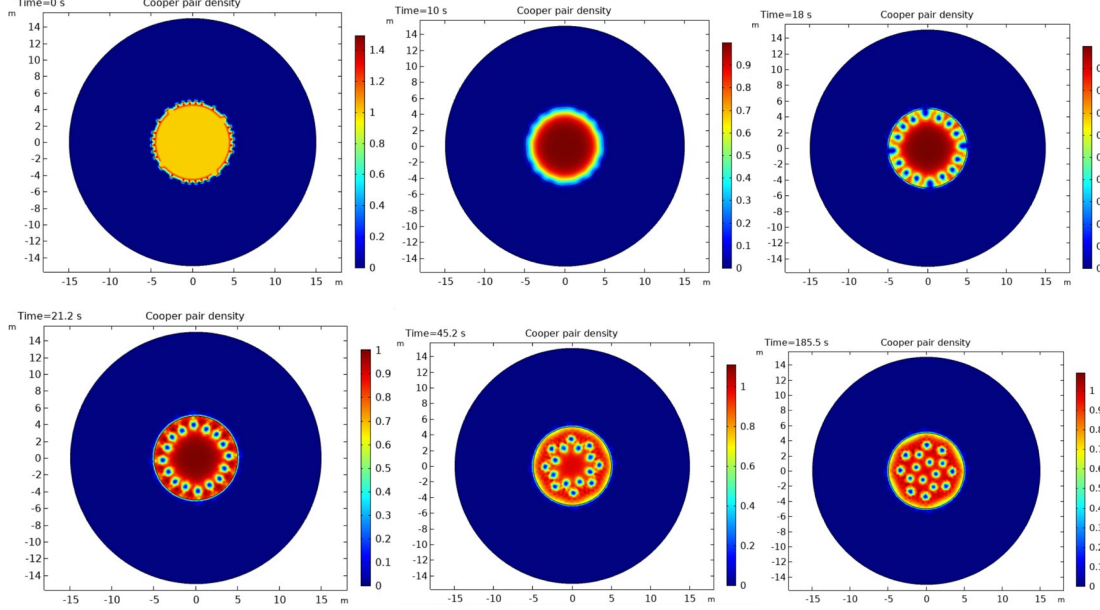


Figure 37 Evolution of the vortices using TDGL Equations with boundary conditions at time  $t=0, 10\text{s}, 18\text{s}, 21.2\text{s}, 65.2\text{s}, 185.5\text{s}$

As the TDGL equations with different boundary conditions are also investigated, the next simulation is current carrying superconducting wires. The interesting part is that for a short period of time the supercurrent becomes negative. The whole process respect to time is shown at figure 38 step by step.

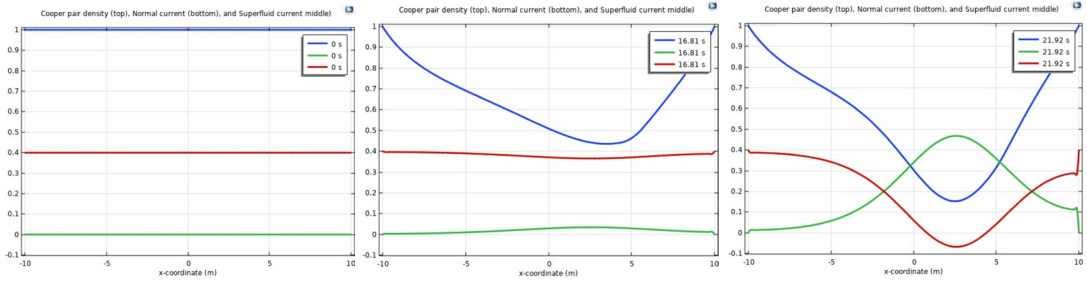


Figure 38 Cooper Pair Density (Top), Normal Current (Bottom) and Supercurrent (Middle) with time at  $t=0, 13.86$  and  $21.92\text{s}$

Thin films are used widely, hence the simulation of the superconducting thin films are also crucial to do. The flowing electric current in superconductors causes vortice patterns and the time evolution of this formation are given at figure 39.

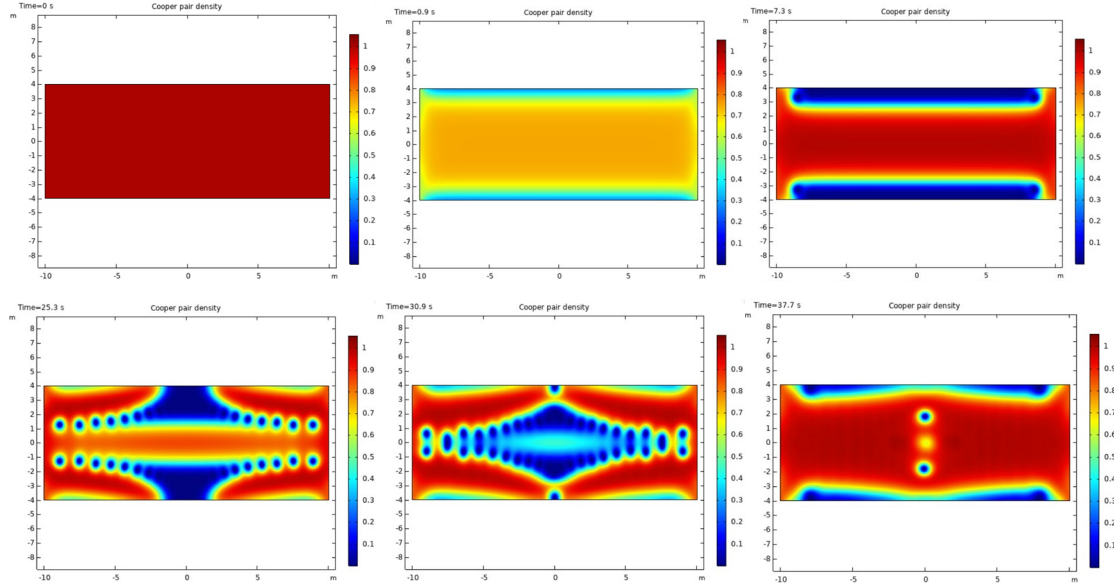


Figure 39 Cooper Pair Density with respect to time at  $t = 0, 0.9s, 1.8s, 21.3s, 30.7s$  and  $37s$

For the generation and cloning of the single flux quantum (SFQ) pulses on superconductor – normal metal – superconductor junctions, the motion of the pulses with cooper pair densities with respect to time is shown at figure 40 step by step.

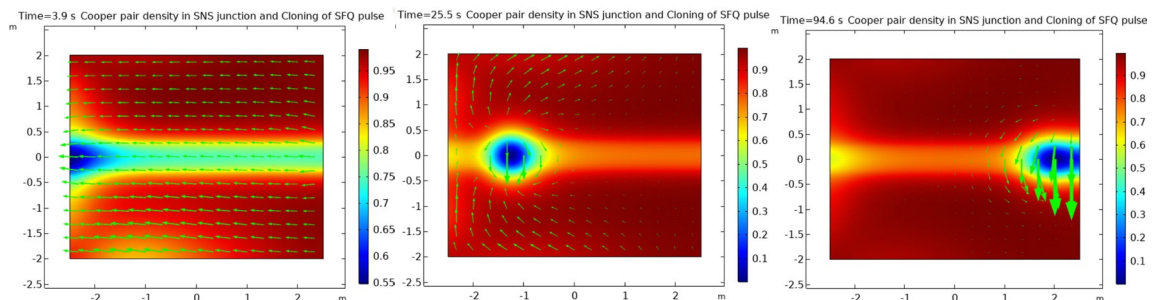


Figure 40 Formation of the SFQ Pulse respect to time

And for the last simulation, qubit with the cavity problem is investigated. For the qubit, transmon qubit is used and for the cavity a coplanar waveguide is made. The electric field map for the coupling is shown at figure 41. At figure 42, the S-Parameters of the system. It can be seen that at resonance frequency all of the energy coupled to the resonator.

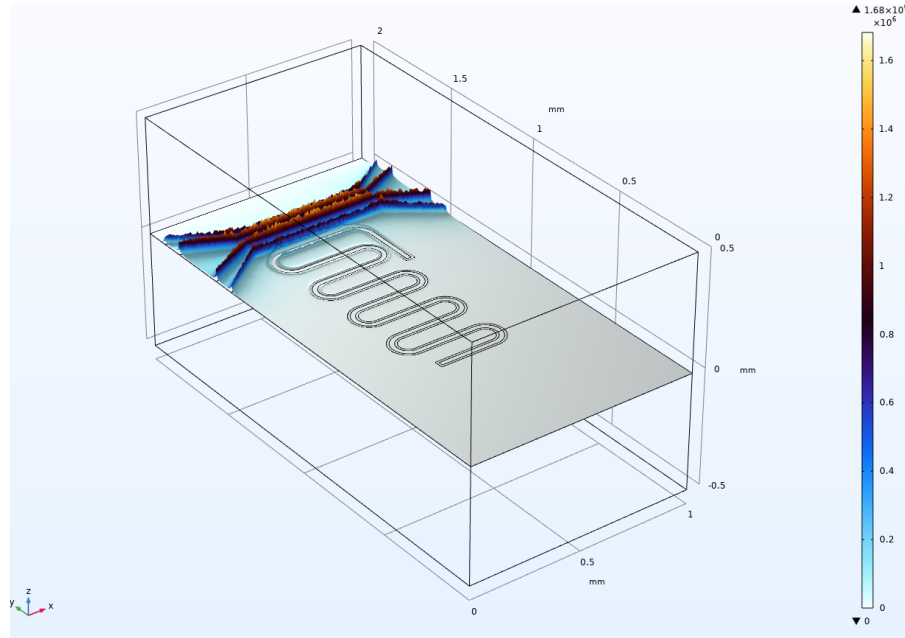


Figure 41 Electric field map of the system

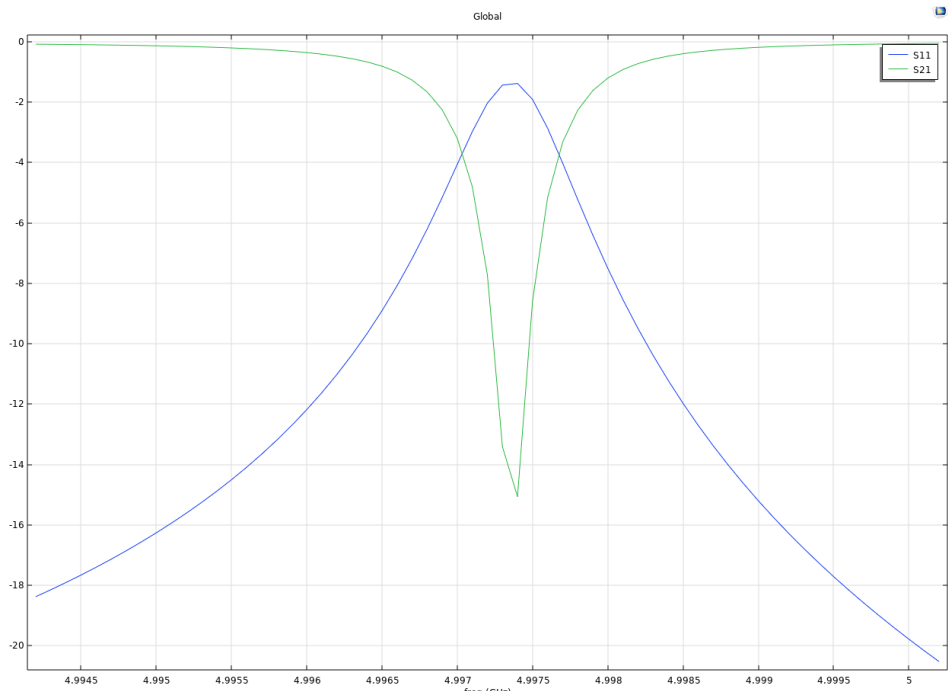


Figure 42 S Parameters of the system

#### **4. CONCLUSION & OUTLOOK**

In conclusion, the power of the simulation software COMSOL Multiphysics prove its capabilities especially in superconductivity simulations. At this thesis, many concepts about superconductivity and their necessary numerical solutions have been investigated.

The results are relatively accurate with the references, however as we have no possibility to check the simulations and compare with the experimental values, the error ratios are not discussed.

On the other hand, creating a qubit in a cavity is challenging and expensive. However, one can make their designs of the both resonator circuit cavity on COMSOL Multiphysics and with the simulations of their design, they may compare different designs respect to their needs and save the cost and time with that.

## 5. REFERENCES

- [1] **H. K. Onnes** (1911). The superconductivity of mercury. *Comm. Phys. Lab. Univ.*
- [2] **Meissner W. and Ochsenfeld R.** (1933) Ein neuer effekt bei eintritt der supraleitfähigkeit. *Naturwissenschaften*, 21:787–788
- [3] **J. Bardeen, L. N. Cooper, and J. R. Schrieffer** (1957), *Phys. Rev.* 106, 162
- [4] **J. Bardeen, L. N. Cooper, and J. R. Schrieffer** (1957), *Phys. Rev.* 108, 1175
- [5] **L. P. Gor'kov** (1959), *Zh. Éksp. Teor. Fiz.* 36, 1918
- [6] **Berglund, P.** (2010), *The glass transition in high-temperature superconductors*. (Dissertation). Retrieved from <http://urn.kb.se/resolve?urn=urn:nbn:se:kth:diva-26388>
- [7] **F. London and H. London** (1935) Proc. Roy. Soc. (London) A149, 71
- [8] **V. L. Ginzburg and L. D. Landau** (1950), *Zh. Éksp. Teor. Fiz.* 20, 1064
- [9] **Gulian, ARMEN** (2021). *Shortcut to superconductivity: Superconducting electronics via Comsol Modeling*. SPRINGER.
- [10] **McKay, D. C., Naik, R., Reinhold, P., Bishop, L. S., & Schuster, D. I.** (2015). High-contrast qubit interactions using multimode cavity QED. *Physical Review Letters*, 114(8). <https://doi.org/10.1103/physrevlett.114.080501>
- [11] **McRae, C. R., Lake, R. E., Long, J. L., Bal, M., Wu, X., Jugderson, B., Metcalf, T. H., Liu, X., & Pappas, D. P.** (2020). Dielectric loss extraction for superconducting microwave resonators. *Applied Physics Letters*, 116(19), 194003. <https://doi.org/10.1063/5.0004622>
- [12] **Pozar, David, M.** (2021). *Microwave engineering*. JOHN WILEY & SONS.
- [13] **Wallraff et. Al.** (2021). *Meter scale Microwave Quantum Networks for Superconducting Circuits*. (Doctoral Dissertation). <http://hdl.handle.net/20.500.11850/527692>
- [14] **Göppl, M., Fragner, A., Baur, M., Bianchetti, R., Filipp, S., Fink, J. M., Leek, P. J., Puebla, G., Steffen, L., & Wallraff, A.** (2008). Coplanar waveguide resonators for circuit quantum electrodynamics. *Journal of Applied Physics*, 104(11), 113904. <https://doi.org/10.1063/1.3010859>

- [15] Houck, A. A., Schreier, J. A., Johnson, B. R., Chow, J. M., Koch, J., Gambetta, J. M., Schuster, D. I., Frunzio, L., Devoret, M. H., Girvin, S. M., & Schoelkopf, R. J. (2008). Controlling the spontaneous emission of a superconducting transmon qubit. *Physical Review Letters*, 101(8). <https://doi.org/10.1103/physrevlett.101.080502>
- [16] Josephson, B. D. (1962). Possible new effects in superconductive tunnelling. *Physics Letters*, 1(7), 251–253. [https://doi.org/10.1016/0031-9163\(62\)91369-0](https://doi.org/10.1016/0031-9163(62)91369-0)
- [17] Ambegaokar, V., & Baratoff, A. (1963). Tunneling between superconductors. *Physical Review Letters*, 11(2), 104–104. <https://doi.org/10.1103/physrevlett.11.104>
- [18] Vool, U., & Devoret, M. (2017). Introduction to quantum electromagnetic circuits. *International Journal of Circuit Theory and Applications*, 45(7), 897–934. <https://doi.org/10.1002/cta.2359>
- [19] Jaynes, E. T., & Cummings, F. W. (1963). Comparison of quantum and semiclassical radiation theories with application to the beam maser. *Proceedings of the IEEE*, 51(1), 89–109. <https://doi.org/10.1109/proc.1963.1664>
- [20] Ryser et. Al. (2014). *Qubit Simulation and Design (Semester Thesis)*.
- [21] Xu, Z., Qian, T., & Sheng, P. (2006). Phase slips in a one-dimensional superconducting wire: Crossover from quantum tunneling to thermal hopping. *Physica C: Superconductivity and Its Applications*, 450(1-2), 118–123. <https://doi.org/10.1016/j.physc.2006.09.005>